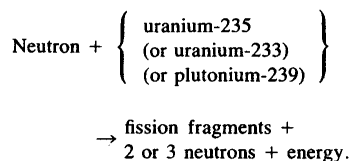


SCIENTIFIC BASIS OF NUCLEAR EXPLOSIONS<sup>2</sup>

## FISSION ENERGY

**1.42** The significant point about the fission of a uranium (or plutonium) nucleus by means of a neutron, in addition to the release of a large quantity of energy, is that the process is accompanied by the instantaneous emission of two or more neutrons; thus,



The neutrons liberated in this manner are able to induce fission of additional uranium (or plutonium) nuclei, each such process resulting in the emission of more neutrons which can produce further fission, and so on. Thus, in principle, a single neutron could start off a chain of nuclear fissions, the number of nuclei suffering fission, and the energy liberated, increasing at a tremendous rate, as will be seen shortly.

**1.43** There are many different ways in which the nuclei of a given fissionable species can split up into two fission fragments (initial fission products), but the total amount of energy liberated per fission does not vary greatly. A satisfactory average value of this energy is 200 million electron volts. The million electron volt (or 1 MeV) unit has been found convenient for expressing the energy released in nuclear reactions; it is

equivalent to  $1.6 \times 10^{-6}$  erg or  $1.6 \times 10^{-13}$  joule. The manner in which this energy is distributed among the fission fragments and the various radiations associated with fission is shown in Table 1.43.

Table 1.43  
DISTRIBUTION OF FISSION ENERGY

	MeV
Kinetic energy of fission fragments	$165 \pm 5$
Instantaneous gamma-ray energy	$7 \pm 1$
Kinetic energy of fission neutrons	$5 \pm 0.5$
Beta particles from fission products	$7 \pm 1$
Gamma rays from fission products	$6 \pm 1$
Neutrinos from fission products	10
Total energy per fission	$200 \pm 6$

**1.44** The results in the table may be taken as being approximately applicable to either uranium-233, uranium-235, or plutonium-239. These are the only three known substances, which are reasonably stable so that they can be stored without appreciable decay, that are capable of undergoing fission by neutrons of all energies. Hence, they are the only materials that can be used to sustain a fission chain. Uranium-238, the most abundant isotope in natural uranium (§ 1.14), and thorium-232 will suffer fission by neutrons of high energy only, but not by those of lower energy. For this reason these substances cannot sustain a chain reaction. However, when fission does occur in these elements, the energy distribution is quite similar to that shown in the table.

**1.45** Only part of the fission energy

<sup>2</sup>The remaining (more technical) sections of this chapter may be omitted without loss of continuity.

## CRITICAL MASS FOR A FISSION CHAIN

is immediately available in a nuclear explosion; this includes the kinetic energy of the fission fragments, most of the energy of the instantaneous gamma rays, which is converted into other forms of energy within the exploding weapon, and also most of the neutron kinetic energy, but only a small fraction of the decay energy of the fission products. There is some compensation from energy released in reactions in which neutrons are captured by the weapon debris, and so it is usually accepted that about 180 MeV of energy are immediately available per fission. There are  $6.02 \times 10^{23}$  nuclei in 235 grams of uranium-235 (or 239 grams of plutonium-239), and by making use of familiar conversion factors (cf. § 1.43) the results quoted in Table 1.45 may be obtained for the energy (and other) equivalents of 1 kiloton of TNT. The calculations are based on an accepted, although somewhat arbitrary, figure of  $10^{12}$  calories as the energy released in the explosion of this amount of TNT.<sup>3</sup>

Table 1.45  
EQUIVALENTS OF 1 KILOTON OF TNT

Complete fission of 0.057 kg (57 grams or 2 ounces) fissionable material
Fission of $1.45 \times 10^{23}$ nuclei
$10^{12}$ calories
$2.6 \times 10^{23}$ million electron volts
$4.18 \times 10^{19}$ ergs ( $4.18 \times 10^{12}$ joules)
$1.16 \times 10^6$ kilowatt-hours
$3.97 \times 10^9$ British thermal units

<sup>3</sup>The majority of the experimental and theoretical values of the explosive energy released by TNT range from 900 to 1,100 calories per gram. At one time, there was some uncertainty as to whether the term "kiloton" of TNT referred to a short kiloton ( $2 \times 10^6$  pounds), a metric kiloton ( $2.205 \times 10^6$  pounds), or a long kiloton ( $2.24 \times 10^6$  pounds). In order to avoid ambiguity, it was agreed that the term "kiloton" would refer to the release of  $10^{12}$  calories of explosive energy. This is equivalent to 1 short kiloton of TNT if the energy release is 1,102 calories per gram or to 1 long kiloton if the energy is 984 calories per gram of TNT.

**1.46** Although two to three neutrons are produced in the fission reaction for every nucleus that undergoes fission, not all of these neutrons are available for causing further fissions. Some of the fission neutrons are lost by escape, whereas others are lost in various non-fission reactions. In order to sustain a fission chain reaction, with continuous release of energy, at least one fission neutron must be available to cause further fission for each neutron previously absorbed in fission. If the conditions are such that the neutrons are lost at a faster rate than they are formed by fission, the chain reaction would not be self-sustaining. Some energy would be produced, but the amount would not be large enough, and the rate of liberation would not be sufficiently fast, to cause an effective explosion. It is necessary, therefore, in order to achieve a nuclear explosion, to establish conditions under which the loss of neutrons is minimized. In this connection, it is especially important to consider the neutrons which escape from the substance undergoing fission.

**1.47** The escape of neutrons occurs at the exterior of the uranium (or plutonium) material. The rate of loss by escape will thus be determined by the surface area. On the other hand, the fission process, which results in the formation of more neutrons, takes place

drawn up into the cloud, only a relatively small proportion of the dirt particles become contaminated with radioactivity. This is because the particles do not mix intimately with the weapon residues in the cloud at the time when the fission products are still vaporized and about to condense. For a burst near the land surface, however, large quantities of dirt and other debris are drawn into the cloud at early times. Good mixing then occurs during the initial phases of cloud formation and growth. Consequently, when the vaporized fission products condense they do so on the foreign matter, thus forming highly radioactive particles (§ 2.23).

**2.11** At first the rising mass of weapon residues carries the particles upward, but after a time they begin to fall slowly under the influence of gravity, at rates dependent upon their size. Consequently, a lengthening (and widening) column of cloud (or smoke) is produced. This cloud consists chiefly of very small particles of radioactive fission products and weapon residues, water droplets, and larger particles of dirt and debris carried up by the after-winds.

**2.12** The speed with which the top of the radioactive cloud continues to ascend depends on the meteorological conditions as well as on the energy yield of the weapon. An approximate indication of the rate of rise of the cloud from a 1-megaton explosion is given by the results in Table 2.12 and the curve in Fig. 2.12. Thus, in general, the cloud will have attained a height of 3 miles in 30 seconds and 5 miles in about a min-

**Table 2.12**  
**RATE OF RISE OF RADIOACTIVE CLOUD  
FROM A 1-MEGATON AIR BURST**

Height (miles)	Time (minutes)	Rate of Rise (miles per hour)
2	0.3	330
4	0.7	270
6	1.1	220
10	2.5	140
12	3.8	77

ute. The average rate of rise during the first minute or so is nearly 300 miles per hour (440 feet per second). These values should be regarded as rough averages only, and large deviations may be expected in different circumstances (see also Figs. 10.158a, b, c).

**2.13** The eventual height reached by the radioactive cloud depends upon the heat energy of the weapon, and upon the atmospheric conditions, e.g., moisture content and stability. The greater the amount of heat generated the greater will be the upward thrust due to buoyancy and so the greater will be the distance the cloud ascends. The maximum height attained by the radioactive cloud is strongly influenced by the tropopause, i.e., the boundary between the troposphere below and the stratosphere above, assuming that the cloud attains the height of the troposphere.<sup>2</sup>

**2.14** When the cloud reaches the tropopause, there is a tendency for it to spread out laterally, i.e., sideways. But if sufficient energy remains in the radioactive cloud at this height, a portion of it will penetrate the tropopause and ascend into the more stable air of the stratosphere.

<sup>2</sup>The tropopause is the boundary between the troposphere and the relatively stable air of the stratosphere. It varies with season and latitude, ranging from 25,000 feet near the poles to about 55,000 feet in equatorial regions (§ 9.128).

the pressure in the blast wave has not fallen below atmospheric, but in the curve marked  $t_0$  it is seen that at some distance behind the shock front the overpressure has a negative value. In this region the air pressure is below that of the original (or ambient) atmosphere, so that an "underpressure" rather than an overpressure exists.

**3.05** During the negative (rarefaction or suction) phase, a partial vacuum is produced and the air is sucked in, instead of being pushed away from the explosion as it is when the overpressure is positive. At the end of the negative phase, which is somewhat longer than the positive phase, the pressure has essentially returned to ambient. The peak (or maximum) values of the underpressure are usually small compared with the peak positive overpressures; the former are generally not more than about 4 pounds per square inch below the ambient pressure whereas the positive overpressure may be much larger. With increasing distance from the explosion, both peak values decrease, the positive more rapidly than the negative,

and they approach equality when the peak pressures have decayed to a very low level.

#### THE DYNAMIC PRESSURE

**3.06** The destructive effects of the blast wave are frequently related to values of the peak overpressure, but there is another important quantity called the "dynamic pressure." For a great variety of building types, the degree of blast damage depends largely on the drag force associated with the strong winds accompanying the passage of the blast wave. The drag force is influenced by certain characteristics—primarily the shape and size—of the structure, but this force also depends on the peak value of the dynamic pressure and its duration at a given location.

**3.07** The dynamic pressure is proportional to the square of the wind velocity and to the density of the air behind the shock front. Both of these quantities may be related to the overpressure under ideal conditions at the wave front by certain equations, which will be given later (see § 3.55). For very

**Table 3.07**

#### PEAK OVERPRESSURE AND DYNAMIC PRESSURE AND MAXIMUM WIND VELOCITY IN AIR AT SEA LEVEL CALCULATED FOR AN IDEAL SHOCK FRONT

Peak overpressure (pounds per square inch)	Peak dynamic pressure (pounds per square inch)	Maximum wind velocity (miles per hour)
200	330	2,078
150	222	1,777
100	123	1,415
72	74	1,168
50	41	934
30	17	669
20	8.1	502
10	2.2	294
5	0.6	163
2	0.1	70

**Table 3.66**  
AVERAGE ATMOSPHERIC DATA FOR MID-LATITUDES

Altitude (feet)	Temperature (degrees Kelvin)	Pressure (psi)	Altitude Scaling Factors			Speed of Sound (ft/sec)
			$S_p$	$S_s$	$S_t$	
0	288	14.70	1.00	1.00	1.00	1,116
1,000	286	14.17	0.96	1.01	1.02	1,113
2,000	284	13.66	0.93	1.03	1.03	1,109
3,000	282	13.17	0.90	1.04	1.05	1,105
4,000	280	12.69	0.86	1.05	1.07	1,101
5,000	278	12.23	0.83	1.06	1.08	1,097
10,000	268	10.11	0.69	1.13	1.17	1,077
15,000	258	8.30	0.56	1.21	1.28	1,057
20,000	249	6.76	0.46	1.30	1.39	1,037
25,000	239	5.46	0.37	1.39	1.53	1,016
30,000	229	4.37	0.30	1.50	1.68	995
35,000	219	3.47	0.24	1.62	1.86	973
40,000	217	2.73	0.19	1.75	2.02	968
45,000	217	2.15	0.15	1.90	2.19	968
50,000	217	1.69	0.12	2.06	2.37	968
55,000	217	1.33	0.091	2.23	2.57	968
60,000	217	1.05	0.071	2.41	2.78	968
65,000	217	0.83	0.056	2.61	3.01	968
70,000	218	0.65	0.044	2.83	3.25	971
75,000	219	0.51	0.035	3.06	3.50	974
80,000	221	0.41	0.028	3.31	3.78	978
85,000	222	0.32	0.022	3.57	4.07	981
90,000	224	0.25	0.017	3.86	4.38	984
95,000	225	0.20	0.014	4.17	4.71	988
100,000	227	0.16	0.011	4.50	5.07	991
110,000	232	0.10	0.0070	5.23	5.82	1,003
120,000	241	0.067	0.0045	6.04	6.61	1,021
130,000	249	0.044	0.0030	6.95	7.47	1,038
140,000	258	0.029	0.0020	7.95	8.41	1,056
150,000	266	0.020	0.0013	9.06	9.43	1,073

**3.67** The correction factors in § 3.66 are applicable for burst altitudes up to about 40,000 feet (about 7.6 miles). Nearly all of the energy from nuclear explosions below this altitude is absorbed by air molecules near the burst. Deviations from the scaling laws described in the preceding paragraphs are caused principally by differences in

the partitioning of the energy components when the burst occurs above 40,000 feet. At such altitudes, part of the energy that would have contributed to the blast wave at lower altitudes is emitted as thermal radiation.

**3.68** To allow for the smaller fraction of the yield that appears as blast energy at higher altitudes, the actual

yield is multiplied by a "blast efficiency factor" to obtain an effective blast yield. There is no simple way to formulate the blast efficiency factor as a function of altitude since, at high altitudes, overpressure varies with distance in such a manner that the effective blast yield is different at different distances. It is possible, however, to specify upper and lower limits on the blast efficiency factor, as shown in Table 3.68 for several altitudes. By using this factor, together with the ambient pressure  $P$  and the absolute temperature  $T$  at the observation point (or target) in the equations in § 3.65 (or § 3.66), an estimate can be made of the upper and lower limits of the blast parameters. An example of such an estimate will be given later.

**Table 3.68**  
BLAST EFFICIENCY FACTORS FOR HIGH-ALTITUDE BURSTS

Burst Altitude (feet)	Blast Efficiency Factor	
	Upper Limit	Lower Limit
40,000	1.0	0.9
60,000	1.0	0.8
90,000	0.9	0.6
120,000	0.7	0.4
150,000	0.4	0.2

#### STANDARD CURVES AND CALCULATIONS OF BLAST WAVE PROPERTIES

**3.69** In order to estimate the damage which might be expected to occur at a particular range from a given explosion, it is necessary to define the characteristics of the blast wave as they vary with time and distance. Consequently, standard "height of burst" curves of the various air blast wave properties are given here to supplement

the general discussion already presented. These curves show the variation of peak overpressure, peak dynamic pressure, arrival time, and positive phase duration with distance from ground zero for various heights of burst over a nearly ideal surface. Similar curves may also be constructed for other blast wave parameters, but the ones presented here are generally considered to be the most useful. They apply to urban targets as well as to a wide variety of other approximately ideal situations.

**3.70** From the curves given below the values of the blast wave properties can be determined for a free air burst or as observed at the surface for an air burst at a particular height or for a contact surface burst (zero height). The peak overpressures, dynamic pressures, and positive phase duration times obtained in this manner are the basic data to be used in determining the blast loading and response of a target to a nuclear explosion under specified conditions. The procedures for evaluating the blast damage to be expected are discussed in Chapters IV and V.

**3.71** The standard curves give the blast wave properties for a 1-kiloton TNT equivalent explosion in a sea-level atmosphere. By means of these curves and the scaling laws already presented, the corresponding properties can be calculated for an explosion of  $W$ -kilotons energy yield. Examples of the use of the curves are given on the pages facing the figures. It should be borne in mind that the data have been computed for nearly ideal conditions and that significant deviations may occur in practice.

**3.72** The variation of peak overpressure with distance from a 1-kiloton TNT equivalent free air burst, i.e., a

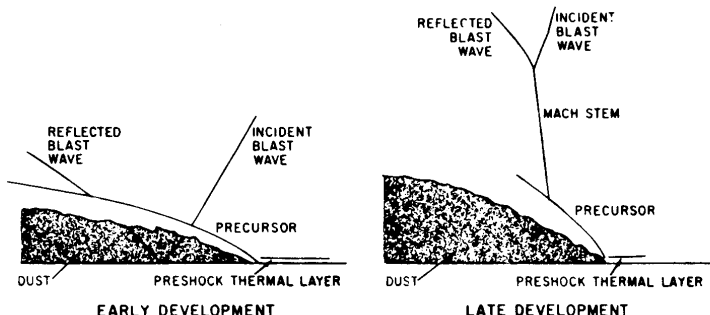


Figure 3.81. Precursor characteristics.

given in Fig. 4.67a.) Dynamic pressure waveforms often have high-frequency oscillations that indicate severe turbulence. Peak amplitudes of the precursor waveforms show that the overpressure has a lower peak value and the dynamic pressure a higher peak value than over a surface that did not permit a precursor to form. The higher peak value of the dynamic pressure is primarily attributable to the increased density of the moving medium as a result of the dust loading in the air. Furthermore, the normal Rankine-Hugoniot relations at the shock front no longer apply.

**3.83** Examples of surfaces which are considered thermally nearly ideal (unlikely to produce significant precursor effects) and thermally nonideal (expected to produce a precursor for suitable combinations of burst height and ground distance) are given in Table 3.83. Under many conditions, e.g., for scaled heights of burst in excess of 800 feet or at large ground distances (where the peak overpressure is less than about 6 psi), precursors are not expected to occur regardless of yield and type of

surface. Thermal effects on the blast wave are also expected to be small for contact surface bursts; consequently, it is believed that in many situations, especially in urban areas, nearly ideal blast wave conditions would prevail.

**3.84** For this reason, the curves for various air blast parameters presented earlier, which apply to nearly ideal surface conditions, are considered to be

Table 3.83

EXAMPLES OF  
THERMALLY NEARLY IDEAL AND  
THERMALLY NONIDEAL SURFACES

Thermally Nearly Ideal (precursor unlikely)	Thermally Nonideal (precursor may occur for low air bursts)
Water	Desert sand
Ground covered by white smoke	Coral
Heat-reflecting concrete	Asphalt
Ice	Surface with thick low vegetation
Packed snow	Surface covered by dark smoke
Moist soil with sparse vegetation	Most agricultural areas
Commercial and industrial areas	Dry soil with sparse vegetation

blast wave enters and tends to equalize the interior and exterior pressures. In fact, a structure may be designed to have certain parts frangible to lessen damage to all other portions of the structure. Thus, the response of certain elements in such cases influences the blast loading on the structure as a whole. In general, the movement of a structural element is not considered to influence the blast loading on that element itself. However, an exception to this rule arises in the case of an aircraft in flight when struck by a blast wave.

## BLAST LOADING-TIME CURVES

**4.38** The procedures whereby curves showing the air blast loading as a function of time may be derived are given below. The methods presented are for the following five relatively simple shapes: (1) closed box-like structure; (2) partially open box-like structure; (3) open frame structure; (4) cylindrical structure; and (5) semicircular arched structure. These methods can be altered somewhat for objects having similar characteristics. For very irregularly shaped structures, however, the proce-

dures described may provide no more than a rough estimate of the blast loading to be expected.

**4.39** As a general rule, the loading analysis of a diffraction-type structure is extended only until the positive phase overpressure falls to zero at the surface under consideration. Although the dynamic pressure persists after this time, the value is so small that the drag force can be neglected. However, for drag-type structures, the analysis is continued until the dynamic pressure is zero. During the negative overpressure phase, both overpressure and dynamic pressure are too small to have any significant effect on structures (§ 3.11 *et seq.*).

**4.40** The blast wave characteristics which need to be known for the loading analysis and their symbols are summarized in Table 4.40. The locations in Chapter III where the data may be obtained, at a specified distance from ground zero for an explosion of given energy yield and height of burst, are also indicated.

**4.41** A closed box-like structure may be represented simply by a parallelepiped, as in Fig. 4.41, having a length  $L$ , height  $H$ , and breadth  $B$ . Structures

Table 4.40

## BLAST WAVE CHARACTERISTICS FOR DETERMINATION OF LOADING

Property	Symbol	Source
Peak overpressure	$p$	Figs. 3.73a, b, and c
Time variation of overpressure	$p(t)$	Fig. 3.57
Peak dynamic pressure	$q$	Fig. 3.75
Time variation of dynamic pressure	$q(t)$	Fig. 3.58
Reflected overpressure	$p_r$	Fig. 3.78b
Duration of positive phase of overpressure	$t_p^*$	Fig. 3.76
Duration of positive phase of dynamic pressure	$t_q^*$	Fig. 3.76
Blast front (shock) velocity	$U$	Fig. 3.55

Table 5.139a

## DAMAGE CRITERIA FOR STRUCTURES PRIMARILY AFFECTED BY DIFFRACTION LOADING

Structural Type	Description of Structure	Description of Damage		
		Severe	Moderate	Light
1	Multistory reinforced concrete building with reinforced concrete walls, blast resistant design for 30 psi Mach region pressure from 1 MT, no windows.	Walls shattered, severe frame distortion, incipient collapse.	Walls breached or on the point of being so, frame distorted, entranceways damaged, doors blown in or jammed, extensive spalling of concrete.	Some cracking of concrete walls and frame.
2	Multistory reinforced concrete building with concrete walls, small window area, three to eight stories.	Walls shattered, severe frame distortion, incipient collapse.	Exterior walls severely cracked. Interior partitions severely cracked or blown down. Structural frame permanently distorted, extensive spalling of concrete.	Windows and doors blown in, interior partitions cracked.
3	Multistory wall-bearing building, brick apartment house type, up to three stories.	Collapse of bearing walls, resulting in total collapse of structure.	Exterior walls severely cracked, interior partitions severely cracked or blown down.	Windows and doors blown in, interior partitions cracked.
4	Multistory wall-bearing building, monumental type, up to four stories.	Collapse of bearing walls, resulting in collapse of structure supported by these walls. Some bearing walls may be shielded by intervening walls so that part of the structure may receive only moderate damage.	Exterior walls facing blast severely cracked, interior partitions severely cracked with damage toward far end of building possibly less intense.	Windows and doors blown in, interior partitions cracked.
5	Wood frame building, house type, one or two stories.	Frame shattered resulting in almost complete collapse.	Wall framing cracked. Roof severely damaged, interior partitions blown down.	Windows and doors blown in, interior partitions cracked.

## ANALYSIS OF DAMAGE FROM AIR BLAST

Table 5.139b

## DAMAGE CRITERIA FOR STRUCTURES PRIMARILY AFFECTED BY DRAG LOADING

Structural Type	Description of Structure	Description of Damage		
		Severe	Moderate	Light
6	Light steel frame industrial building, single story, with up to 5-ton crane capacity; low strength walls which fail quickly.	Severe distortion or collapse of frame.	Minor to major distortion of frame; cranes, if any, not operable until repairs made.	Windows and doors blown in, light siding ripped off.
7	Heavy steel-frame industrial building, single story, with 25 to 50-ton crane capacity; lightweight, low strength walls which fail quickly.	Severe distortion or collapse of frame.	Some distortion to frame; cranes not operable until repairs made.	Windows and doors blown in, light siding ripped off.
8	Heavy steel frame industrial building, single story, with 60 to 100-ton crane capacity; lightweight low strength walls which fail quickly.	Severe distortion or collapse of frame.	Some distortion or frame; cranes not operable until repairs made.	Windows and doors blown in, light siding ripped off.
9	Multistory steel-frame office-type building, 3 to 10 stories. Lightweight low strength walls which fail quickly, earthquake resistant construction.	Severe frame distortion, incipient collapse.	Frame distorted moderately, interior partitions blown down.	Windows and doors blown in, light siding ripped off, interior partitions cracked.
10	Multistory steel-frame office-type building, 3 to 10 stories. Lightweight low strength walls which fail quickly, non-earthquake resistant construction.	Severe frame distortion, incipient collapse.	Frame distorted moderately, interior partitions blown down.	Windows and doors blown in, light siding ripped off, interior partitions cracked.

## STRUCTURAL DAMAGE FROM AIR BLAST

Table 5.139b (continued)

Structural Type	Description of Structure	Description of Damage		
		Severe	Moderate	Light
11	Multistory reinforced concrete frame office-type building, 3 to 10 stories; lightweight low strength walls which fail quickly, earthquake resistant construction.	Severe frame distortion, incipient collapse.	Frame distorted moderately, interior partitions blown down, some spalling of concrete.	Windows and doors blown in, light siding ripped off, interior partitions cracked.
12	Multistory reinforced concrete frame office type building, 3 to 10 stories; lightweight low strength walls which fail quickly, non-earthquake resistant construction.	Severe frame distortion, incipient collapse.	Frame distorted moderately, interior partitions blown down, some spalling of concrete.	Windows and doors blown in, light siding ripped off, interior partitions cracked.
13	Highway truss bridges, 4-lane, spans 200 to 400 ft; railroad truss bridges, double track ballast floor, spans 200 to 400 ft.	Total failure of lateral bracing or anchorage, collapse of bridge.	Substantial distortion of lateral bracing or slippage on supports, significant reduction in capacity of bridge.	Capacity of bridge not significantly reduced, slight distortion of some bridge components.
14	Highway truss bridges, 2-lane, spans 200 to 400 ft; railroad truss bridges, single track ballast or double track open floors, spans 200 to 400 ft; railroad truss bridges, single track open floor, span 400 ft.	(Ditto)	(Ditto)	(Ditto)
15	Railroad truss bridges, single track open floor, span 200 ft.	(Ditto)	(Ditto)	(Ditto)
16	Highway girder bridges, 4-lane through, span 75 ft.	(Ditto)	(Ditto)	(Ditto)

## ANALYSIS OF DAMAGE FROM AIR BLAST

Table 5.139b (concluded)

Structural Type	Description of Structure	Description of Damage		
		Severe	Moderate	Light
17	Highway girder bridges, 2-lane deck, 2-lane through, 4-lane deck, span 75 ft; railroad girder bridges, double-track deck, open or ballast floor, span 75 ft; railroad girder bridges, single or double track through, ballast floors, span 75 ft.	(Ditto)	(Ditto)	(Ditto)
18	Railroad girder bridges, single track deck, open or ballast floors, span 75 ft; railroad girder bridges, single or double track through, open floors, span 75 ft.	(Ditto)	(Ditto)	(Ditto)
19	Highway girder bridges, 2-lane through, 4-lane deck or through, span 200 ft; railroad girder bridges, double track deck or through, ballast floor, span 200 ft.	(Ditto)	(Ditto)	(Ditto)
20	Highway girder bridges, 2-lane deck, span 200 ft; railroad girder bridges, single track deck or through, ballast floors, span 200 ft; railroad girder bridges, double track deck or through, open floors, span 200 ft.	(Ditto)	(Ditto)	(Ditto)
21	Railroad girder bridges, single track deck or through, open floors, span 200 ft.	(Ditto)	(Ditto)	(Ditto)

**Table 5.145****CONDITIONS OF FAILURE OF OVERPRESSURE-SENSITIVE ELEMENTS**

Structural element	Failure	Approximate side-on peak overpressure (psi)
Glass windows, large and small.	Shattering usually, occasional frame failure.	0.5- 1.0
Corrugated asbestos siding.	Shattering.	1.0- 2.0
Corrugated steel or aluminum paneling.	Connection failure followed by buckling.	1.0- 2.0
Brick wall panel, 8 in. or 12 in. thick (not reinforced).	Shearing and flexure failures.	3.0-10.0
Wood siding panels, standard house construction.	Usually failure occurs at the main connections allowing a whole panel to be blown in.	1.0- 2.0
Concrete or cinder-block wall panels, 8 in. or 12 in. thick (not reinforced).	Shattering of the wall.	1.5- 5.5

ground zero. For panels that are oriented so that there are no reflected pressures thereon, the side-on pressures must be doubled. The fraction of the area of a panel wall that contains windows will influence the overpressure required to damage the panel. Such damage is a function of the net load, which may be reduced considerably if the windows fail early. This allows the pressure to become equalized on the two sides of the wall before panel failure occurs.

**DRAG-SENSITIVE TARGETS**

**5.146** A diagram of damage-distance relationships for various targets which are largely affected by drag forces is given in Fig. 5.146. The conditions under which it is applicable and the

limits of accuracy are similar to those in § 5.141 and § 5.142, respectively; the possibility of fire mentioned in § 5.144 must also be kept in mind. The targets (Items 1 to 13) in the figure are enumerated on the page facing Fig. 5.146 and the different types of damage are described in the following paragraphs.

*Transportation Equipment*

**5.147** The damage criteria for various types of land transportation equipment, including civilian motor-driven vehicles and earth-moving equipment, and railroad rolling stock are given in Table 5.147a. The various types of damage to merchant shipping from air blast are described in Table 5.147b.

(Text continued on page 225.)

**Table 5.147a****DAMAGE CRITERIA FOR LAND TRANSPORTATION EQUIPMENT**

Description of equipment	Damage	Nature of damage
Motor equipment (cars and trucks).	Severe	Gross distortion of frame, large displacements, outside appurtenances (doors and hoods) torn off, need rebuilding before use.
	Moderate	Turned over and displaced, badly dented, frames sprung, need major repairs.
	Light	Glass broken, dents in body, possibly turned over, immediately usable.
Railroad rolling stock (box, flat, tank, and gondola cars).	Severe	Car blown from track and badly smashed, extensive distortion, some parts usable.
	Moderate	Doors demolished, body damaged, frame distorted, could possibly roll to repair shop.
	Light	Some door and body damage, car can continue in use.
Railroad locomotives (Diesel or steam).	Severe	Overturned, parts blown off, sprung and twisted, major overhaul required.
	Moderate	Probably overturned, can be towed to repair shop after being righted, need major repairs.
	Light	Glass breakage and minor damage to parts, immediately usable.
Construction equipment (bulldozers and graders).	Severe	Extensive distortion of frame and crushing of sheet metal, extensive damage to caterpillar tracks and wheels.
	Moderate	Some frame distortion, overturning, track and wheel damage.
	Light	Slight damage to cabs and housing, glass breakage.

**Table 5.147b****DAMAGE CRITERIA FOR SHIPPING FROM AIR BLAST**

Damage type	Nature of damage
Severe	The ship is either sunk, capsized, or damaged to the extent of requiring rebuilding.
Moderate	The ship is immobilized and requires extensive repairs, especially to shock-sensitive components or their foundations, e.g., propulsive machinery, boilers, and interior equipment.
Light	The ship may still be able to operate, although there will be damage to electronic, electrical, and mechanical equipment.

*Communication and Power Lines*

**5.148** Damage to telephone, telegraph, and utility power lines is generally either severe or light. Such damage depends on whether the poles supporting the lines are damaged or not. If the poles are blown down, damage to the lines will be severe and extensive repairs will be required. On the other hand, if the poles remain standing, the lines will suffer only light damage and will need little repair. In general, lines extending radially from ground zero are less susceptible to damage than are those running at right angles to this direction.

*Forests*

**5.149** The detailed characteristics of the damage to forest stands resulting from a nuclear explosion will depend on a variety of conditions, e.g., deciduous or coniferous trees, degree of foliation of the trees, natural or planted stands, and favorable or unfavorable growing

conditions. A general classification of forest damage, applicable in most cases, is given in Table 5.149. Trees are primarily sensitive to the drag forces from a blast wave and so it is of interest that the damage in an explosion is similar to that resulting from a strong, steady wind; the velocities of such winds that would produce comparable damage are included in the table.

**5.150** The damage-distance results derived from Fig. 5.146 apply in particular to unimproved coniferous forests which have developed under unfavorable growing conditions and to most deciduous forests in the temperate zone when foliation is present. Improved coniferous forests, with trees of uniform height and a smaller average tree density per acre, are more resistant to blast than are unimproved forests which have grown under unfavorable conditions. A forest of defoliated deciduous trees is also somewhat more blast resistant than is implied by the data in Fig. 5.146.

Table 5.149

## DAMAGE CRITERIA FOR FORESTS

Damage type	Nature of damage	Equivalent steady wind velocity (miles per hour)
Severe	Up to 90 percent of trees blown down; remainder denuded of branches and leaves. (Area impassable to vehicles and very difficult on foot.)	130-140
Moderate	About 30 percent of trees blown down; remainder have some branches and leaves blown off. (Area passable to vehicles only after extensive clearing.)	90-100
Light	Only applies to deciduous forest stands. Very few trees blown down; some leaves and branches blown off. (Area passable to vehicles.)	60-80

## PARKED AIRCRAFT

**5.151** Aircraft are relatively vulnerable to air blast effects associated with nuclear detonations. The forces developed by peak overpressures of 1 to 2 pounds per square inch are sufficient to dash in panels and buckle stiffeners and stringers. At higher overpressures, the drag forces due to wind (dynamic) pressure tend to rotate, translate, overturn, or lift a parked aircraft, so that damage may then result from collision with other aircraft, structures, or the ground. Aircraft are also very susceptible to damage from flying debris carried by the blast wave.

**5.152** Several factors influence the degree of damage that may be expected for an aircraft of a given type at a specified range from a nuclear detonation. Aircraft that are parked with the

nose pointed toward the burst will suffer less damage than those with the tail or either side directed toward the oncoming blast wave (§ 5.94). Shielding of one aircraft by another or by structures or terrain features may reduce damage, especially that caused by flying debris. Standard tiedown of aircraft, as used when high winds are expected, will also minimize the extent of damage at ranges where destruction might otherwise occur.

**5.153** The various damage categories for parked transport airplanes, light liaison airplanes, and helicopters are outlined in Table 5.153 together with the approximate peak overpressures at which the damage may be expected to occur. The aircraft are considered to be parked in the open at random orientation with respect to the point of burst. The

Table 5.153

## DAMAGE CRITERIA FOR PARKED AIRCRAFT

Damage type	Nature of damage	Overpressure (psi)
Severe	Major (or depot level) maintenance required to restore aircraft to operational status.	Transport airplanes 3 Light liaison craft 2 Helicopters 3
Moderate	Field maintenance required to restore aircraft to operational status.	Transport airplanes 2 Light liaison craft 1 Helicopters 1.5
Light	Flight of the aircraft not prevented, although performance may be restricted.	Transport airplanes 1.0 Light liaison craft 0.75 Helicopters 1.0

deformation that the earth provides to flexible structures by the buttressing action of the soil.

**5.158** For lightweight, shallow buried underground structures the top of the earth cover is at least flush with the original grade but the depth of cover is not more than 6 percent of the span. Such structures are not sufficiently deep for the ratio of the depth of burial to the span to be large enough to obtain the benefits described in § 5.161. The soil provides little attenuation of the air blast pressure applied to the top surface of a shallow buried underground structure. Observations made at full-scale nuclear tests indicate that there is apparently no increase in pressure on the structure as a result of ground shock reflection at the

interface between the earth and the top of the structure.

**5.159** The lateral blast pressures exerted on the vertical faces of a shallow buried structure have been found to be as low as 15 percent of the blast pressure on the roof in dry, well-compacted, silty soils. For most soils, however, this lateral blast pressure is likely to be somewhat higher and may approach 100 percent of the roof blast pressure in porous saturated soil. The pressures on the bottom of a buried structure, in which the bottom slab is a structural unit integral with the walls, may range from 75 to 100 percent of the pressure exerted on the roof.

**5.160** The damage that might be suffered by a shallow buried structure

**Table 5.160**  
DAMAGE CRITERIA FOR SHALLOW BURIED STRUCTURES

Type of structure	Damage type	Peak over-pressure (psi)	Nature of damage
Light, corrugated steel arch, surface structure (10-gage corrugated steel with a span of 20–25 ft), central angle of 180°; 5 ft of earth cover at the crown.*	Severe Moderate	45– 60 50– 50	Collapse Large deformations of end walls and arch, also major entrance door damage.
Buried concrete arch 8-in. thick with a 16 ft span and central angle of 180°; 4 ft of earth cover at the crown.	Severe Moderate	220–280 100–220	Collapse. Large deformations with considerable cracking and spalling.
	Light	30– 40	Damage to ventilation and entrance door.
	Light	120–160	Cracking of panels, possible entrance door damage.

\*For arched structures reinforced with ribs, the collapse pressure is higher depending on the number of ribs.

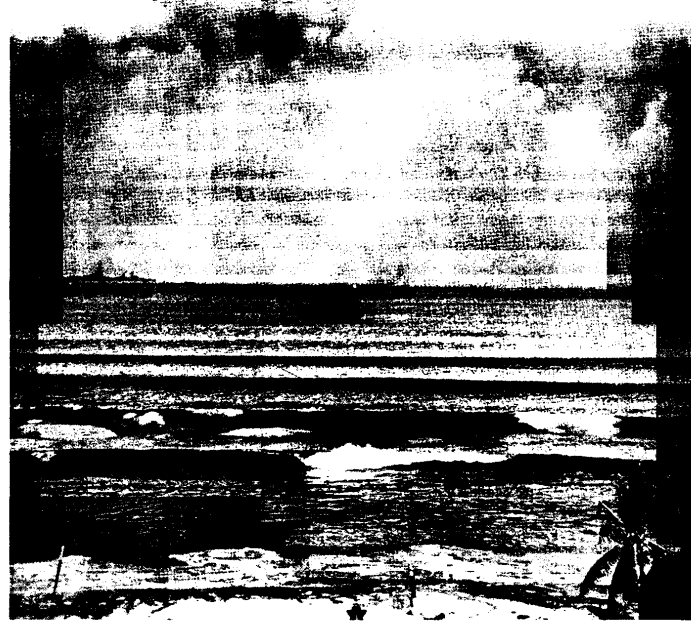


Figure 6.55. Waves from the BAKER underwater explosion reaching the beach at Bikini, 11 miles from surface zero.

**Table 6.57**  
MAXIMUM HEIGHTS (CREST TO TROUGH) AND ARRIVAL TIMES OF WATER WAVES AT BIKINI BAKER TEST

Distance (yards)	330	660	1,330	2,000	2,700	3,300	4,000
Wave height (feet)	94	47	24	16	13	11	9
Time (seconds)	11	23	48	74	101	127	154

at the Bikini BAKER test. A more generalized treatment of wave heights, which can be adapted to underwater explosions of any specified energy, is given in § 6.119 *et seq.*

**6.58** For the conditions that existed in the BAKER test, water wave damage

is possible to ships that are moderately near to surface zero. There was evidence for such damage to the carrier U.S.S. Saratoga, anchored in Bikini lagoon almost broadside on to the explosion with its stern 400 yards from surface zero. The "island" structure was

**Table 6.108**  
DAMAGE CRITERIA FOR MODERATELY DEEP UNDERGROUND STRUCTURES

Structural Type	Damage Type	Distance from Surface Zero	Nature of Damage
Relatively small, heavy, well-designed, underground structures.	Severe	1½ apparent crater radii	Collapse.
	Light	2½ apparent crater radii	Slight cracking, severance of brittle external connections.
Relatively long, flexible structures, e.g., buried pipelines, tanks, etc.	Severe	1½ apparent crater radii	Deformation and rupture.
	Moderate	2 apparent crater radii	Slight deformation and rupture.
	Light	2½ to 3 apparent crater radii	Failure of connections.

operative by the shock. Such equipment may be made less vulnerable by suitable shock mounting. Shock mounts (or shock isolators) are commonly made of an elastic material like rubber or they may consist of springs. The material absorbs much of the energy delivered very rapidly by the shock and releases it more slowly, thereby protecting the mounted equipment.

**6.113** By shaking, vibrating, or dropping pieces of equipment, engineers can often estimate the vulnerabil-

ity of that equipment to all kinds of motion. The results are commonly expressed as the natural vibration frequency at which the equipment is most vulnerable and the maximum acceleration tolerable at that frequency for 50 percent probability of severe damage. Some examples of the values of these parameters for four classes of equipment, without and with shock mounting, are quoted in Table 6.113. It is seen that the shock mounting serves to decrease the most sensitive natural fre-

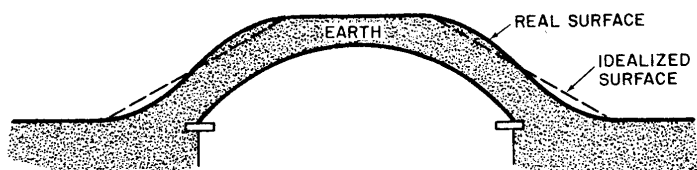


Figure 6.111. Configuration of mounded arch.

**Table 6.113**  
FREQUENCY AND VULNERABILITY ACCELERATION OF TYPICAL EQUIPMENT ITEMS

Class	Item	Shock Mounted	Typical Value of	
			Natural frequency (cps)	Vulnerability acceleration (g)
A	Heavy machinery—motors, generators, transformers, etc. (>4000 lb).	No	10	20
		Yes	3	40
B	Medium and light machinery—pumps, condensers, air conditioning, fans, small motors (<1000 lb).	No	20	40
		Yes	5	80
C	Communication equipment, relays, rotating magnetic drum units of electronic equipment, etc.	No	25	7
		Yes	6	60
D	Storage batteries, piping and duct work.	No	20	70
		Yes	5	150

quency, i.e., increase the period, and to increase the acceleration for 50 percent probability of severe damage at that frequency.

**6.114** Whether or not a specified piece of equipment is likely to be damaged by a particular ground motion can be estimated from the data in Table 6.113 in conjunction with the response spectrum (§ 6.90) for that ground mo-

tion. If the peak acceleration on the response spectrum corresponding to the equipment frequency is less than the vulnerability acceleration, then the equipment will probably be undamaged by the particular ground motion. On the other hand, if the response spectrum indicates that the equipment may be damaged, shock mounting should be added or improved.

#### TECHNICAL ASPECTS OF UNDERWATER BURSTS

##### SHOCK WAVE PROPERTIES

**6.115** By combining a theoretical treatment with measurements made in connection with detonations of high-explosive charges under water, some characteristic properties of the underwater shock wave from a nuclear ex-

plosion have been calculated. The peak pressure of the shock wave in water for various energy yields is shown in Fig. 6.115 as a function of slant range,  $R$ , for pressures less than 3,000 pounds per square inch and (in the top right corner) as a function of the scaled slant range,

Table 7.35

## APPROXIMATE RADIANT EXPOSURES FOR IGNITION OF FABRICS FOR LOW AIR BURSTS

Material	Weight (oz/yd <sup>2</sup> )	Color	Effect on Material	Radiant Exposure* (cal/cm <sup>2</sup> )		
				35 kilotons	1.4 megatons	20 megatons
<b>CLOTHING FABRICS</b>						
Cotton	8	White	Ignites	32	48	85
		Khaki	Tears on flexing	17	27	34
		Khaki	Ignites	20	30	39
		Olive	Tears on flexing	9	14	21
		Olive	Ignites	14	19	21
		Dark blue	Tears on flexing	11	14	17
		Dark blue	Ignites	14	19	21
Cotton corduroy	8	Brown	Ignites	11	16	22
Cotton denim, new	10	Blue	Ignites	12	27	44
Cotton shirting	3	Khaki	Ignites	14	21	28
Cotton-nylon mixture	5	Olive	Tears on flexing	8	15	17
		Olive	Ignites	12	28	53
Wool	8	White	Tears on flexing	14	25	38
		Khaki	Tears on flexing	14	24	34
		Olive	Tears on flexing	9	13	19
		Dark blue	Tears on flexing	8	12	18
	20	Dark blue	Tears on flexing	14	20	26
Rainwear (double neoprene-coated nylon twill)	9	Olive	Begins to melt	5	9	13
		Olive	Tears on flexing	8	14	22
<b>DRAPEY FABRICS</b>						
Rayon gabardine	6	Black	Ignites	9	20	26
Rayon-acetate drapery	5	Wine	Ignites	9	22	28
Rayon gabardine	7	Gold	Ignites	**	24†	28†
Rayon twill lining	3	Black	Ignites	7	17	25
Rayon twill lining	3	Beige	Ignites	13	20	28
Acetate-shantung	3	Black	Ignites	10†	22†	35†
Cotton heavy draperies	13	Dark colors	Ignites	15	18	34
<b>TENT FABRICS</b>						
Canvas (cotton)	12	White	Ignites	13	28	51
Canvas	12	Olive drab	Ignites	12	18	28
<b>OTHER FABRICS</b>						
Cotton chenille bedspread		Light blue	Ignites	**	11†	15†
Cotton venetian blind tape, dirty		White	Ignites	10	18	22
Cotton venetian blind tape		White	Ignites	13†	27†	31†
Cotton muslin window shade	8	Green	Ignites	7	13	19

\*Radiant exposures for the indicated responses (except where marked †) are estimated to be valid to  $\pm 25\%$  under standard laboratory conditions. Under typical field conditions the values are estimated to be valid within  $\pm 50\%$  with a greater likelihood of higher rather than lower values. For materials marked †, ignition levels are estimated to be valid within  $\pm 50\%$  under laboratory conditions and within  $\pm 100\%$  under field conditions.

\*\*Data not available or appropriate scaling not known.

Table 7.40

## APPROXIMATE RADIANT EXPOSURES FOR IGNITION OF VARIOUS MATERIALS FOR LOW AIR BURSTS

Material	Weight (oz/yd <sup>2</sup> )	Color	Effect on Material	Radiant Exposure* (cal/cm <sup>2</sup> )		
				35 kilotons	1.4 megatons	20 megatons
<b>HOUSEHOLD TINDER MATERIALS</b>						
Newspaper, shredded	2		Ignites	4	6	11
Newspaper, dark picture area	2		Ignites	5	7	12
Newspaper, printed text area	2		Ignites	6	8	15
Crepe paper	1	Green	Ignites	6	9	16
Kraft paper	3	Tan	Ignites	10	13	20
Bristol board, 3 ply	10	Dark	Ignites	16	20	40
Kraft paper carton, used (flat side)	16	Brown	Ignites	16	20	40
New bond typing paper	2	White	Ignites	24†	30†	50†
Cotton rags		Black	Ignites	10	15	20
Rayon rags		Black	Ignites	9	14	21
Cotton string scrubbing mop (used)		Gray	Ignites	10†	15†	21†
Cotton string scrubbing mop (weathered)		Cream	Ignites	10†	19†	26†
Paper book matches, blue head exposed			Ignites	11†	14†	20†
Excelsior, ponderosa pine	2 lb/ft <sup>2</sup>	Light yellow	Ignites	**	23†	23†
<b>OUTDOOR TINDER MATERIALS***</b>						
Dry rotted wood punk (fir)			Ignites	4†	6†	8†
Deciduous leaves (beech)			Ignites	4	6	8
Fine grass (cheat)			Ignites	5	8	10
Coarse grass (sedge)			Ignites	6	9	11
Pine needles, brown (ponderosa)			Ignites	10	16	21
<b>CONSTRUCTION MATERIALS</b>						
Roll roofing, mineral surface			Ignites	**	>34	>116
Roll roofing, smooth surface			Ignites	**	30	77
Plywood, douglas fir			Flaming during exposure	9	16	20
Rubber, pale latex			Ignites	50	80	110
Rubber, black			Ignites	10	20	25
<b>OTHER MATERIALS</b>						
Aluminum aircraft skin (0.020 in. thick) coated with 0.002 in. of standard white aircraft paint			Blisters	15	30	40
Cotton canvas sandbags, dry filled			Failure	10	18	32
Coral sand			Explodes (popcorning)	15	27	47
Siliceous sand			Explodes (popcorning)	11	19	35

\*Radiant exposures for the indicated responses (except where marked †) are estimated to be valid to  $\pm 25\%$  under standard laboratory conditions. Under typical field conditions the values are estimated to be valid within  $\pm 50\%$  with a greater likelihood of higher rather than lower values. For materials marked †, ignition levels are estimated to be valid within  $\pm 50\%$  under laboratory conditions and within  $\pm 100\%$  under field conditions.

\*\*Data not available or appropriate scaling not known.

\*\*\*Radiant exposures for ignition of these substances are highly dependent on the moisture content.

Table 7.85

## ATMOSPHERIC DENSITY RATIOS

Altitude (feet)	Density Ratio, $\rho(h)/\rho_0$	Altitude (feet)	Density Ratio, $\rho(h)/\rho_0$
15,000	0.63	60,000	0.095
20,000	0.53	65,000	0.075
25,000	0.45	70,000	0.059
30,000	0.37	75,000	0.046
35,000	0.31	80,000	0.036
40,000	0.24	85,000	0.028
45,000	0.19	90,000	0.022
50,000	0.15	95,000	0.017
55,000	0.12	100,000	0.014

desired. For a contact surface burst (§ 2.127 footnote) the fireball develops in a manner approaching that for an air burst of twice the yield, because the blast wave energy is reflected back from the surface into the fireball (§ 3.34). Hence,  $t_{\max}$  may be expected to be larger than for an air burst of the same actual yield.

7.86 The thermal power curve in Fig. 7.84 (left scale) presents some features of special interest. As is to be expected, the thermal power (or rate of emission of radiant energy) of the fireball rises to a maximum, just as does the temperature in the second radiation pulse. However, since the thermal power is roughly proportional to  $T^4$ , it increases and decreases much more rapidly than does the temperature. This accounts for the sharp rise to the maximum in the  $P/P_{\max}$  curve, followed by a somewhat less sharp drop which tapers off as the fireball approaches its final stages. The amount of thermal energy,  $E$ , emitted by the fireball in an air burst up to any specified time can be obtained from the area under the curve of  $P/P_{\max}$

versus  $t/t_{\max}$  up to that time. The results, expressed as  $E/E_{\text{tot}}$  (percent) versus  $t/t_{\max}$ , are shown by the second curve (right scale) in Fig. 7.84, where  $E_{\text{tot}}$  is the total thermal energy emitted by the fireball. It is seen that at a time equal to 10  $t_{\max}$  about 80 percent of the thermal energy will have been emitted; hence this time may be taken as a rough measure of the effective duration of the thermal pulse for an air burst. Since  $t_{\max}$  increases with the explosion energy yield, so also does the pulse length.

7.87 The fact that the thermal pulse length increases with the weapon yield has a bearing on the possibility of people taking evasive action against thermal radiation. Evasive action is expected to have greater relative effectiveness for explosions of higher than lower yield because of the longer thermal pulse duration. The situation is indicated in another way in Fig. 7.87, which shows the thermal energy emission as a function of actual time, rather than of  $t/t_{\max}$ , for four different explosion energy yields. The data were derived from the corresponding curve in Fig. 7.84 by using the

## TECHNICAL ASPECTS OF THERMAL RADIATION

appropriate calculated value of  $t_{\max}$  for each yield. At the lower energy yields the thermal radiation is emitted in such a short time that no evasive action is possible. At the higher yields, however, exposure to much of the thermal radiation could be avoided if evasive action were taken within a fraction of a second of the explosion time. It must be remembered, of course, that even during this short period a very considerable amount of thermal energy will have been emitted from an explosion of high yield.

7.88 The fraction of the explosion energy yield in the form of thermal radiation, i.e.,  $E_{\text{tot}}/W$ , is called the "thermal partition" and is represented

by the symbol  $f$ . Estimated values of  $f$  are given in Table 7.88 for air bursts with yields in the range from 1 kiloton to 10 megatons at altitudes up to 100,000 feet (19 miles). The data for heights of burst up to 15,000 feet were obtained primarily from experimental results. For higher bursts altitudes, the values were obtained by calculations, various aspects of which were checked with experimental results. They are considered to be fairly reliable for yields between 1 kiloton and 1 megaton at altitudes up to 50,000 feet (9.5 miles). Outside this range of yields and altitudes, the data in Table 7.88 may be used with less confidence. Values of  $f$  for burst altitudes above 100,000 feet are given in § 7.90 (see also § 7.104).

Table 7.88

## THERMAL PARTITION FOR VARIOUS EXPLOSION YIELDS AT DIFFERENT ALTITUDES

Height of Burst (kilofeet)	Thermal Partition, $f$				
	1	10	100	1,000	10,000
Up to 15	0.35	0.35	0.35	0.35	0.35
20	0.35	0.36	0.39	0.41	0.43
30	0.35	0.36	0.39	0.41	0.43
40	0.35	0.36	0.38	0.40	0.42
50	0.35	0.36	0.38	0.40	0.42
60	0.35	0.37	0.38	0.40	0.42
70	0.36	0.37	0.39	0.40	0.42
80	0.37	0.38	0.39	0.41	0.43
90	0.38	0.39	0.40	0.41	0.43
100	0.40	0.40	0.41	0.42	0.45

cloud layer and a snow covered surface, the correction is  $1.5 \times 1.5 = 2.25$ .

#### SURFACE BURSTS

**7.101** For a surface burst, the radiant exposures along the earth's surface will be less than for equal distances from an air burst of the same total yield. This difference arises partly, as indicated in § 7.20, from the decreased transmittance of the intervening low air layer due to dust and water vapor produced by the explosion. Furthermore, the normal atmosphere close to the earth's surface transmits less than at higher altitudes. In order to utilize the equations in § 7.96 to determine radiant exposure for surface bursts, the concept of an "effective thermal partition" is used, together with the normal transmittance, such as given in Fig. 7.98, for the existing atmospheric conditions.

Based upon experimental data, contact surface bursts can be represented fairly well by an effective thermal partition of 0.18. Values of the thermal partition for other surface bursts are shown in Table 7.101; they have been derived by assigning a thermal partition of 0.18 to a contact surface burst and interpolating between that value and the air burst thermal partition values in Table 7.88.

#### VERY-HIGH-ALTITUDE BURSTS

**7.102** In the calculation of the thermal radiation exposure at the surface of the earth from very-high-altitude nuclear explosions, two altitude regions must be considered because of the change in the fireball behavior that occurs at altitudes in the vicinity of about 270,000 feet (§ 7.91). At burst heights from roughly 160,000 to 200,000 feet (30 to 38 miles), the ther-

Table 7.101  
EFFECTIVE THERMAL PARTITION FOR SURFACE BURSTS

Height of Burst (feet)	Thermal Partition				
	Total Yield (kilotons)				
	1	10	100	1,000	10,000
20	0.19	*	*	*	*
40	0.21	0.19	*	*	*
70	0.23	0.21	0.19	*	*
100	0.26	0.22	0.20	*	*
200	0.35	0.25	0.21	0.19	*
400	**	0.33	0.25	0.21	0.19
700	**	**	0.28	0.24	0.21
1,000	**	**	0.34	0.26	0.22
2,000	**	**	**	0.34	0.26
4,000	**	**	**	**	0.33
7,000	**	**	**	**	0.35

\*These may be treated as contact surface bursts, with  $f = 0.18$ .

\*\*Air bursts; for values of  $f$  see Table 7.88.

#### GAMMA RAYS

From Fig. 8.33a, the dose for the case specified is seen to be somewhat less than 300 rads. A reasonable interpolated value would appear to be about 250 rads.

**8.35** The data in Figs. 8.33a and b are dependent upon the density of the air between the center of the explosion and the point on the ground at which the radiation is received. This is so because the air absorbs some of the gamma radiation in the course of its transmission; the dense air near the surface absorbs more than the less dense air at higher altitudes. If the actual average density is higher or lower than 0.9 of the normal sea-level value for which the curves were drawn, the gamma-ray dose will be decreased or increased, respectively.

**8.36** It will be noted, especially in Fig. 8.33b, that for a specified dose, the slant range increases more rapidly in the higher explosion yield range, i.e., the slope of the curves becomes steeper. The cause is the sustained low air density following the passage of the positive phase of the shock wave (§ 3.04), particularly for explosions of high energy yield. The emission of gamma rays by the fission products is delayed (§ 8.13) and so these radiations do not

reach distant points until the shock wave has passed and the air density has decreased. There is consequently less attenuation of the fission product gamma rays by the air than at lower energy yields. This effect is known as the "hydrodynamic enhancement" of the gamma-ray dose.

**8.37** The foregoing figures were calculated for heights of burst of  $200 W^{0.4}$  feet and the conclusions are reasonably applicable provided the height of burst exceeds about 300 feet, even though the fireball may touch the earth's surface. For a contact surface burst (§ 2.127 footnote) the dose for a specified explosion yield and range may be obtained upon multiplication of the corresponding dose in Fig. 8.33a or b by a factor which depends to some extent on both yield and range. The factors in Table 8.37 for some specific yields are averages which provide a fair approximation for distances of interest. The factors for intermediate yields may be obtained by interpolation. Interpolation between unity and the tabulated factor may also be used to obtain the appropriate factors for bursts between about 300 feet and the actual surface.

Table 8.37  
CORRECTION FACTORS FOR CONTACT SURFACE BURSTS

Fig. 8.33a		Fig. 8.33b	
Yield	Factor	Yield	Factor
1 to 50 KT	%	100 KT	1
100 KT	1	300 KT	1 1/4
		700 KT	1 1/2
		2 MT	2
		5 to 20 MT	3

shield the attenuation is generally greater than indicated by the effective tenth-value thickness and so use of the latter would be conservative.

8.41 The effective tenth-value thicknesses of some materials of interest in radiation shielding are given in Table 8.41,<sup>7</sup> for broad beams of gamma rays emitted by the fission products in the first minute after the detonation and for those (secondary gamma rays) accompanying the capture of neutrons by nitrogen in the air (§ 8.11). These particular radiations were chosen because they are representative of the main constituents of the initial gamma rays. The thickness of any material required to decrease the nitrogen capture (secondary) gamma rays to one-tenth is about 50 percent greater than for the fission product gamma rays; this is because the former have a considerably higher energy.

Table 8.41

## APPROXIMATE EFFECTIVE TENTH-VALUE THICKNESSES FOR FISSION PRODUCT AND NITROGEN CAPTURE GAMMA RAYS

Material	Fission Product			Nitrogen Capture	
	Density (lb/cu ft)	Tenth- Value Thickness (inches)	$D \times T$ (lb/sq ft)	Tenth- Value Thickness (inches)	$D \times T$ (lb/sq ft)
Steel (Iron)	490	3.3	135	4.3	176
Concrete	146	11	134	16	194
Earth	100	16	133	24	200
Water	62.4	24	125	39	201
Wood	40	38	127	63	210

<sup>7</sup>The tenth-value thicknesses are for gamma rays that are incident perpendicularly on the slab of material. If the rays make an angle  $\theta$  with the perpendicular, the tenth-value thickness is obtained approximately by multiplying the values in the table by cosine  $\theta$ , provided  $\theta$  is less than 45°.

## TRANSIENT-RADIATION EFFECTS ON ELECTRONICS (TREE)

Table 8.72

## DOSE TRANSMISSION FACTORS FOR VARIOUS STRUCTURES

Structure	Initial Gamma Rays	Neutrons
Three feet underground	0.002-0.004	0.002-0.01
Frame House	0.8-1.0	0.3-0.8
Basement	0.1-0.6	0.1-0.8
Multistory building (apartment type):		
Upper stories	0.8-0.9	0.9-1.0
Lower stories	0.3-0.6	0.3-0.8
Concrete blockhouse shelter:		
9-in. walls	0.1-0.2	0.3-0.5
12-in. walls	0.05-0.1	0.2-0.4
24-in. walls	0.007-0.02	0.1-0.2
Shelter, partly above grade:		
With 2 ft earth cover	0.03-0.07	0.02-0.08
With 3 ft earth cover	0.007-0.02	0.01-0.05

## TRANSIENT-RADIATION EFFECTS ON ELECTRONICS (TREE)

## GENERAL CHARACTERISTICS OF TREE

8.73 The initial nuclear radiation, specifically gamma rays and neutrons, can affect materials, such as those used in electronics systems, e.g., radio and radar sets, gyroscopes, inertial guidance devices, computers, etc. The response of such systems to radiation from a nuclear explosion depends on the nature of the radiation absorbed and also on the specific component and often on the operating state of the system. The actual effects are determined by the characteristics of the circuits contained in the electronics package, the exact components present in the circuits, and the specific construction techniques and materials used in making the components.

8.74 The name commonly applied to the class of effects under consideration is "transient-radiation effects on electronics," commonly abbreviated to the acronym TREE. In general, TREE means those effects occurring in an electronics system as a result of exposure to the transient initial radiation from a nuclear weapon explosion. The adjective "transient" applies to the radiation since it persists for a short time, i.e., less than 1 minute. The response, however, is not necessarily transient. In order to study the effects of nuclear radiations on electronics systems and components, the transient radiation from a weapon is simulated in the laboratory by means of controlled sources of both steady-state and transient radiations.

**Table 8.96**  
LINEAR ATTENUATION COEFFICIENTS FOR GAMMA RAYS

Gamma-ray Energy (MeV)	Linear Attenuation Coefficient ( $\mu$ ) in $\text{cm}^{-1}$				
	Air	Water	Concrete	Iron	Lead
0.5	$1.11 \times 10^{-4}$	0.097	0.22	0.66	1.64
1.0	$0.81 \times 10^{-4}$	0.071	0.15	0.47	0.80
2.0	$0.57 \times 10^{-4}$	0.049	0.11	0.33	0.52
3.0	$0.46 \times 10^{-4}$	0.040	0.088	0.28	0.47
4.0	$0.41 \times 10^{-4}$	0.034	0.078	0.26	0.48
5.0	$0.35 \times 10^{-4}$	0.030	0.071	0.25	0.52
10	$0.26 \times 10^{-4}$	0.022	0.060	0.23	0.55

**8.97** By suitable measurements and theoretical calculations, it is possible to determine the separate contributions of the Compton effect ( $\mu_c$ ), of the photoelectric effect ( $\mu_p$ ), and of pair production ( $\mu_{pp}$ ) to the total linear attenuation coefficient as functions of the gamma-ray energy. The results for lead, a typical heavy element (high atomic number) with a large attenuation coefficient, are given in Fig. 8.97a and those for air, a mixture of light elements (low atomic number) with a small attenuation coefficient, in Fig. 8.97b. Except at extremely low energies, the photoelectric effect in air is negligible, and hence is not shown in the figure. At the lower gamma-ray energies, the linear attenuation coefficients in both lead and air decrease with increasing energy because of the decrease in the Compton and photoelectric effects. At energies in ex-

cess of 1.02 MeV, pair production begins to make an increasingly significant contribution. Therefore, at sufficiently high energies the attenuation coefficient begins to increase after passing through a minimum. This is apparent in Fig. 8.97a, as well as in the last column of Table 8.96, for lead. For elements of lower atomic weight, the increase does not set in until very high gamma-ray energies are attained, e.g., about 17 MeV for concrete and 50 MeV for water.

**8.98** The fact that the attenuation coefficient decreases as the gamma-ray energy increases, and may pass through a minimum, has an important bearing on the problem of shielding. For example, a shield intended to attenuate gamma rays of 1 MeV energy will be much less effective for radiations of 10 MeV energy because of the lower value of the

**Table 9.19**  
RELATIVE THEORETICAL DOSE RATES FROM EARLY FALLOUT AT VARIOUS TIMES AFTER A NUCLEAR EXPLOSION

Time (hours)	Relative dose rate	Time (hours)	Relative dose rate
1	1,000	36	15
1½	610	48	10
2	400	72	6.2
3	230	100	4.0
5	130	200	1.7
6	100	400	0.69
10	63	600	0.40
15	40	800	0.31
24	23	1,000	0.24

known, by actual measurement, the value at any other time can be estimated. All that is necessary is to compare the ratios (to the unit-time reference dose rate) for the two given times as obtained from Fig. 9.16a or Fig. 9.16b. For example, suppose the dose rate at 3 hours after the explosion is found to be 50 rads/hr; what would be the value at 18 hours? The respective ratios, as given by the curve in Fig. 9.16a, are 0.23 and 0.033, with respect to the unit-time reference dose rate. Hence, the dose rate at 18 hours after the explosion is  $50 \times 0.033 / 0.23 = 7.2$  rads/hr.

**9.19** The results in Figs. 9.16a and b may be represented in an alternative form, as in Table 9.19, which is more convenient, although somewhat less complete. The dose rate, in any suitable units, is taken as 1,000 at 1 hour after a nuclear explosion; the expected dose rate in the same units at a number of subsequent times, for the same quantity of early fallout, are then as given in the

table. If the actual dose rate at 1 hour (or any other time) after the explosion is known, the value at any specified time, up to 1,000 hours, can be obtained by simple proportion.<sup>4</sup>

**9.20** It should be noted that Figs. 9.16a and b and Table 9.19 are used for calculations of dose rates. In order to determine the total or accumulated radiation dose received during a given period it is necessary to multiply the average dose rate by the exposure time. However, since the dose rate is steadily decreasing during the exposure, appropriate allowance for this must be made. The results of the calculations based on Fig. 9.16a are expressed by the curve in Fig. 9.20. It gives the total dose received from early fallout, between 1 minute and any other specified time after the explosion, in terms of the unit-time reference dose rate.

**9.21** To illustrate the application of Fig. 9.20, suppose that an individual becomes exposed to a certain quantity of gamma radiation from early fallout 2

<sup>4</sup>Devices, similar to a slide rule, are available for making rapid calculations of the decay of fallout dose rates and related matters.

Table 9.22

## PERCENTAGES OF INFINITE TIME RESIDUAL RADIATION DOSE RECEIVED FROM 1 MINUTE UP TO VARIOUS TIMES AFTER EXPLOSION

Time (hours)	Percent of infinite time dose	Time (hours)	Percent of infinite time dose
1	55	72	86
2	62	100	88
4	68	200	90
6	71	500	93
12	75	1,000	95
24	80	2,000	97
48	83	10,000	99

**9.24** With the aid of Figs. 9.16a and b and Fig. 9.20 (or the equivalent Tables 9.19 and 9.22) many different types of calculations relating to radiation dose rates and total doses received from early fallout can be made. The procedures can be simplified, however, by means of special charts, as will be shown below. The results, like those already given, are applicable to a particular quantity of fallout. If there is any change in the situation, either by further contamination or by decontamination, the conclusions will not be valid.

**9.25** If the radiation dose rate from early fallout is known at a given location, the nomograph in Fig. 9.25 may be used to determine the dose rate at any

other time at the same location, assuming there has been no change in the fallout other than natural radioactive decay. The same nomograph can be utilized, alternatively, to determine the time after the explosion at which the dose rate will have attained a specified value. The nomograph is based on the straight line marked " $t^{-1.2}$ " in Figs. 9.16a and b which is seen to deviate only slightly from the continuous decay curve for times less than 6 months or so. It is thus possible to obtain from Fig. 9.25 approximate dose rates, which are within 25 percent of the continuous curve values of Figs. 9.16a and b for the first 200 days after the nuclear detonation.

(Text continued on page 404.)

## RADIOACTIVE CONTAMINATION FROM NUCLEAR EXPLOSION

The base surge is influenced strongly by the wind, moving as an entity at the existing wind speed and direction. Initially, the base surge is highly radioactive, but as it expands and becomes diluted the concentration of fission products, etc., decreases. This dispersion, coupled with radioactive decay, results in comparatively low dose rates from the base surge by about 30 minutes after the burst (§ 2.77 *et seq.*).

**9.55** The radioactivity in the water is initially present in a disk-like "pool," usually not more than 300 feet deep, near the ocean surface which is moved by the local currents. The pool gradually expands into a roughly annular form, but it reverts to an irregular disk shape at later times. Eventually, downward mixing and horizontal turbulent diffusion result in a rapid dilution of the radioactivity, thus reducing the hazard with time.

**9.56** In the Bikini BAKER test (§ 2.63), the contaminated fallout (or rainout) consisted of both solid particles and a slurry of sea salt crystals in drops of water. This contamination was difficult to dislodge and had there been per-

sonnel on board the ships used in the test, they would have been subjected to considerable doses of radiation if the fallout were not removed immediately.<sup>6</sup> Since the BAKER shot was fired in shallow water, the bottom material may have helped in the scavenging of the radioactive cloud, thus adding to the contamination. It is expected that for shallow bursts in very deep water the fallout from the cloud will be less than observed at the test in Bikini lagoon.

**9.57** An indication of the rate of spread of the active material and the decrease in the dose rate following a shallow underwater burst is provided by the data in Table 9.57, obtained after the Bikini BAKER test. Although the dose rate in the water was still fairly high after 4 hours, there would be considerable attenuation in the interior of a ship, so that during the time required to cross the contaminated area the total dose received would be small. Within 2 or 3 days after the BAKER test the radioactivity had spread over an area of about 50 square miles, but the radiation dose rate in the water was so low that the region could be traversed in safety.

Table 9.57

## DIMENSIONS AND DOSE RATE IN CONTAMINATED WATER AFTER THE 20-KILOTON UNDERWATER EXPLOSION AT BIKINI

Time after explosion (hours)	Contaminated area (square miles)	Mean diameter (miles)	Maximum dose rate (rads/hr)
4	16.6	4.6	3.1
38	18.4	4.8	0.42
62	48.6	7.9	0.21
86	61.8	8.9	0.042
100	70.6	9.5	0.025
130	107	11.7	0.008
200	160	14.3	0.0004

<sup>6</sup>The technique of washdown of ships, by continuous flow of water over exposed surfaces to remove fallout as it settles, was developed as a result of the Bikini BAKER observations.

**Table 9.74a**  
ESTIMATED RAINFALL DURATION FOR RAINOUT

Percent of Cloud Scavenged	Duration of Rainfall (hours)
25	0.07
50	0.16
75	0.32
90	0.53
99	1.1

**Table 9.74b**  
ESTIMATED RAINFALL DURATION FOR WASHOUT

Percent of Cloud Scavenged	Duration of Rainfall (hours)		
	Light	Moderate	Heavy
25	8	1.6	0.8
50	19	3.8	1.9
75	38	7.7	3.6
90	64	13	6.4
99	128	26	13

#### FALLOUT PATTERNS

**9.75** Information concerning fallout distribution has been obtained from observations made during nuclear weapons tests at the Nevada Test Site and the Eniwetok Proving Grounds.<sup>7</sup> However, there are many difficulties in the analysis and interpretation of the results, and in their use to predict the situation that might arise from a land surface burst over a large city. This is particularly the case for the megaton-range detonations

at the Eniwetok Proving Grounds. Since the fallout descended over vast areas of the Pacific Ocean, the contamination pattern of a large area had to be inferred from a relatively few radiation dose measurements (§ 9.105). Furthermore, the presence of sea water affected the results, as will be seen below.

**9.76** Nuclear tests in the atmosphere in Nevada have been confined to weapons having yields below 100 kilotons and most of the detonations were from the tops of steel towers 100 to 700

<sup>7</sup>The Eniwetok Proving Grounds, called the Pacific Proving Ground before 1955, included test sites on Bikini and Eniwetok Atolls and on Johnston and Christmas Islands in the Pacific Ocean.

**Table 9.93**

SCALING RELATIONSHIPS FOR UNIT-TIME REFERENCE DOSE-RATE CONTOURS  
FOR A CONTACT SURFACE BURST WITH A YIELD OF  $W$  KILOTONS AND A 15 MPH  
WIND

Reference dose rate (rads/hr)	Downwind distance (statute miles)	Maximum width (statute miles)	Ground zero width (statute miles)
3,000	0.95 $W^{0.45}$	0.0076 $W^{0.36}$	0.026 $W^{0.58}$
1,000	1.8 $W^{0.45}$	0.036 $W^{0.76}$	0.060 $W^{0.57}$
300	4.5 $W^{0.45}$	0.13 $W^{0.66}$	0.20 $W^{0.48}$
100	8.9 $W^{0.45}$	0.38 $W^{0.60}$	0.39 $W^{0.42}$
30	16 $W^{0.45}$	0.76 $W^{0.56}$	0.53 $W^{0.41}$
10	24 $W^{0.45}$	1.4 $W^{0.53}$	0.68 $W^{0.41}$
3	30 $W^{0.45}$	2.2 $W^{0.50}$	0.89 $W^{0.41}$
1	40 $W^{0.45}$	3.3 $W^{0.48}$	1.5 $W^{0.41}$

#### SCALING FOR EFFECTIVE WIND

**9.96** The effective wind speed and direction vary with the heights of the top and bottom of the stabilized cloud (§ 9.84). For a weapon of given yield, these heights will depend upon many factors, including the density and relative humidity of the atmosphere and the altitude of the tropopause. Nevertheless, within the accuracy of the idealized unit-time reference dose-rate contours, approximate values of the cloud heights may be used. The curves in Fig. 9.96 are based on the same model as was used in deriving the dose-rate contours and scaling relationships in § 9.93. They may be taken to be representative of the average altitudes to which nuclear clouds from surface (or low air) bursts of various yields might be expected to rise in the mid-latitudes, e.g., over the United States.

**9.97** If there is no directional shear, then doubling the effective wind speed would cause the particles of a given size that originate at a particular location

within the cloud to reach the ground at twice the distance from ground zero, so that they are spread over roughly twice the area. However, particles of many different sizes will arrive at any given point on the ground as a result of the different travel times from different points of origin in the large nuclear cloud. Consequently, simple scaling relationships for wind speed are not possible. Examination of test data and the results of calculations with computer codes suggest the following approximate scaling procedure: for effective wind speeds of  $v$  miles per hour, the downwind distances derived from Table 9.93 are multiplied by the factor  $F$ , where

$$F = 1 + \frac{v - 15}{60}$$

for effective wind speeds greater than 15 miles per hour, and

$$F = 1 + \frac{v - 15}{30}$$

gible, although there would probably have been many cases of sickness resulting in temporary incapacity.

**9.108** The period of 96 hours after the explosion, for which Fig. 9.105 gives the accumulated radiation doses, was chosen somewhat arbitrarily. It should be understood, however, as has been frequently stated earlier in this chapter, that the radiations from the fallout will continue to be emitted for a long time, although at a gradually decreasing rate. The persistence of the external gamma radiation may be illustrated in connection with the BRAVO test by considering the situation at two different locations in Rongelap Atoll. Fallout began about 4 to 6 hours after the explosion and continued for several hours at both places.

**9.109** The northwestern tip of the atoll, 100 miles from the point of detonation, received 3,300 rads during the first 96 hours after the fallout started. This was the heaviest fallout recorded at the same distance from the explosion and may possibly have represented a hot spot, as mentioned above. About 25 miles south, and 115 miles from ground zero, the dose over the same period was

only 220 rads. The inhabitants of Rongelap Atoll were in this area, and were exposed to radiation dosages up to 175 rads before they were evacuated some 44 hours after the fallout began (§§ 12.124, 12.156). The maximum theoretical exposures in these two areas of the atoll for various time intervals after the explosion, calculated from the decay curves given earlier in this chapter, are recorded in Table 9.109.

**9.110** It must be emphasized that the calculated values in Table 9.109 represent the maximum doses at the given locations, since they are based on the assumption that exposed persons remain out-of-doors for 24 hours each day and that no measures are taken to remove radioactive contamination. Furthermore, no allowance is made for weathering or the possible dispersal of the particles by winds. For example, the dose rates measured on parts of the Marshall Islands on the 25th day following the explosion were found to be about 40 percent of the expected values. Rains were known to have occurred during the second week, and these were probably responsible for the major decrease in the contamination.

Table 9.109

CALCULATED RADIATION DOSES AT TWO LOCATIONS IN RONGELAP ATOLL  
FROM FALLOUT FOLLOWING THE MARCH 1, 1954 TEST AT BIKINI

Exposure period after the explosion	Accumulated dose in this period (rads)	
	Inhabited location	Uninhabited location
First 96 hours . . . . .	220	3,300
96 hours to 1 week . . . . .	35	530
1 week to 1 month . . . . .	75	1,080
1 month to 1 year . . . . .	75	1,100
Total to 1 year . . . . .	405	6,010
1 year to infinity . . . . .	About 8	About 115

radiation in various structures have been made, based partly on calculations and partly on measurements with simulated fallout.

**9.120** Some of the results of these estimates are given in Table 9.120 in terms of a dose-transmission factor (§ 8.72). Ranges of values are given in view of the uncertainties in the estimates themselves and the variations in the degree of shielding that may be obtained at different locations within a structure. (Shielding data for the same structures for initial nuclear radiation are given in Table 8.72.) All of the structures are assumed to be isolated, so that possible effects of adjacent buildings have been neglected. For vehicles, such as auto-

mobiles, buses, trucks, etc., the transmission factor is about 0.5 to 0.7. Rough estimates can thus be made of the shielding from fallout radiation that might be expected in various situations. Depending upon his location, a person in the open in a built-up city area would receive from about 20 to 70 percent of the dose that would be delivered by the same quantity of fallout in the absence of the buildings. An individual standing against a building in the middle of a block would receive a much smaller dose than one standing at the intersection of two streets. In contaminated agricultural areas, the gamma-ray dose above the surface can be reduced by turning over the soil so as to bury the fallout particles.

Table 9.120  
FALLOUT GAMMA-RAY DOSE TRANSMISSION FACTORS FOR VARIOUS STRUCTURES

Structure	Dose transmission factor
Three feet underground	0.0002
Frame house	0.3-0.6
Basement	0.05-0.1
Multistory building (apartment type):	
Upper stories	0.01
Lower stories	0.1
Concrete blockhouse shelter:	
9-in. walls	0.007-0.09
12-in. walls	0.001-0.03
24-in. walls	0.0001-0.002
Shelter, partly above grade:	
With 2 ft earth cover	0.005-0.02
With 3 ft earth cover	0.001-0.005

present purpose. Typical variations of electron density with altitude and with time of day are illustrated in Fig. 10.09. The approximate altitudes of the three main regions of the ionosphere are given in Table 10.09.

Table 10.09

## APPROXIMATE ALTITUDES OF REGIONS IN THE IONOSPHERE

Region	Approximate Altitude (miles)
D	30-55
E	55-95
F	Above 95

**10.10** Although the D-, E-, and F-regions always exist in the daytime and the E- and F-regions at night, the details of the dependence of the electron density on altitude, especially in the F-region, vary with the season, with the geographic latitude, with the solar (sunspot) activity, and with other factors. The curves in Fig. 10.09 are applicable to summer, at middle latitudes, around the time of maximum sunspot activity. The effects of the variable factors mentioned above are fairly well known, so that the corresponding changes in the electron density-altitude curve can be predicted reasonably accurately.

**10.11** In addition to these systematic variations in the electron density, there are temporary changes arising from special circumstances, such as solar flares and magnetic storms. Solar flares can cause a ten-fold increase in the electron density in the D-region, but that in the F-region generally increases by no more than a factor of two. Magnetic storms, on the other hand, produce most

## RADIO AND RADAR EFFECTS

of their effect in the F-region. In some latitudes, the maximum electron density in the ionosphere during a magnetic storm may decrease to some 6 to 10 percent of its normal value.

**10.12** Apart from these major changes in electron density, the causes of which are known, there are other variations that are not well understood. Sometimes an irregular and rapidly varying increase in the electron density is observed in the E-region. Apparently one or more layers of high electron density are formed and they extend over distances of several hundred miles. This is referred to as the "sporadic-E" phenomenon. A somewhat similar effect, called "spread-F," in which there are rapid changes of electron density in space and time, occurs in the F-region. The areas affected by spread-F are generally much smaller than those associated with sporadic-E.

## CHARACTERISTICS OF THE IONOSPHERE

**10.13** The composition of the atmosphere, especially at the higher altitudes, varies with the time of day and with the degree of solar activity; however, a general description that is applicable to daytime conditions and mean sunspot activity is sufficient for the present purpose. Near the earth's surface, the principal constituents of the atmosphere are molecular nitrogen ( $N_2$ ) and molecular oxygen ( $O_2$ ). These diatomic gases continue to be the dominant ones up to an altitude of approximately 75 miles. At about 55 miles, ultraviolet radiation from the sun begins to dissociate the oxygen molecules into two atoms of oxygen ( $O$ ). The extent of

## IONIZATION PRODUCED BY NUCLEAR EXPLOSIONS

Table 10.29  
APPROXIMATE STOPPING ALTITUDES FOR PRINCIPAL WEAPON OUTPUTS CAUSING IONIZATION

Weapon Output	Stopping Altitude (miles)
Prompt radiation	
X rays	35 to 55
Neutrons and gamma rays	15
Debris ions	70
Delayed radiation	
Gamma rays	15
Beta particles	35

tially opaque to all ionizing radiations. The radiation will penetrate only a fairly short distance into the atmosphere before most of its energy is absorbed in causing ionization (or is transformed into other kinds of energy). As the altitude of the explosion increases to 15 miles and above, the radiation can escape to increasingly greater distances. Once the stopping altitude for a given ionizing radiation is reached, the atmosphere above the burst is relatively transparent to that radiation, which can then travel upward and outward to great distances.

**10.31** Below the stopping altitude, in a region of uniform density, the nominal penetration distance of ionizing radiation of a particular kind and energy is inversely proportional to the air density. (The penetration distance is often expressed in terms of the mean free path, as described in § 2.113.) For a particular radiation of a single energy traveling through an undisturbed region of constant density, the penetration distance (or mean free path) can be calculated relatively easily. For a radiation spectrum covering a range of energies and for complex paths along which the air density changes, the computations

are more laborious. For a disturbed atmosphere, calculations of the penetration distance are difficult and not very reliable.

## LOCATION OF RESULTANT IONIZATION

**10.32** The region of maximum energy deposition is the location where ion-pair production is the greatest, but it is not always the location of the maximum density of free electrons. At altitudes below about 30 miles, i.e., at relatively high air densities, removal processes are so rapid that the average lifetime of a free electron is a fraction of a second. An extremely high ion-pair production rate is then required to sustain even a few free electrons per cubic centimeter. But in the D-region (starting at about 30 miles altitude) removal processes are not so rapid and higher electron densities are possible. For the delayed gamma rays, for example, the stopping altitude, i.e., the region of maximum energy deposition and ion-pair production rate, is 15 miles; however, the resultant electron density tends to a maximum at a higher altitude in the D-region.

## RADIO AND RADAR EFFECTS

radar systems, changes in the propagation direction due to refraction can cause angular errors. Moreover, if a radar signal is scattered back to the receiver, it can mask desired target returns or, depending on the characteristics of the scattering medium, it may generate a false target (§ 10.120 *et seq.*).

## RADIO COMMUNICATIONS SYSTEMS

**10.89** The general category of radio systems of interest includes those in which electromagnetic waves are reflected or scattered from the troposphere (§ 9.126) or the ionosphere. Such systems are used primarily for long-distance communications; however, other uses, e.g., over-the-horizon radars, also fall in this category.

**10.90** Detailed analysis of communications systems, even for the normal atmosphere, is difficult and depends largely on the use of empirical data. Measurements made during nuclear tests have shown that both degradation and enhancement of signals can occur. The limited information available, however, has been obtained in tests for

weapon yields and detonation altitudes which were not necessarily those that would maximize the effects on communications systems.

**10.91** It is convenient to discuss radio system effects in accordance with the conventional division of the radio-frequency spectrum into decades of frequency ranges. These ranges, with associated frequencies and wavelengths, are given in Table 10.91. Radar systems, which normally employ the frequency range of VHF or higher, are treated separately in § 10.114 *et seq.*

## VERY-LOW-FREQUENCY RANGE (3 to 30 kHz)

**10.92** The frequencies in the VLF band are low enough for fewer than 100 free electrons/cm<sup>3</sup> to cause reflection of the signal (§ 10.20). The bottom of the ionosphere thus effectively acts as a sharp boundary which is not penetrated, and the electromagnetic radiation is confined between the earth and the ionosphere by repeated reflections. The resulting "sky wave," as it is called, may be regarded as traveling along a duct (or

Table 10.91  
RADIOFREQUENCY SPECTRUM

Name of Range	Frequency Range*	Wavelength Range
Very Low Frequency	VLF	3–30 kHz
Low Frequency	LF	30–300 kHz
Medium Frequency	MF	300–3,000 kHz
High Frequency	HF	3–30 MHz
Very High Frequency	VHF	30–300 MHz
Ultra High Frequency	UHF	300–3,000 MHz
Super High Frequency	SHF	3–30 GHz
Extremely High Frequency	EHF	30–300 GHz

\*The abbreviation kHz, MHz, and GHz refer to kilohertz ( $10^3$  cycles/sec), megahertz ( $10^6$  cycles/sec), and gigahertz ( $10^9$  cycles/sec), respectively.

## RADIO AND RADAR EFFECTS

Table 10.122  
EFFECTS OF NUCLEAR DETONATIONS ON RADIO AND RADAR SYSTEMS

Frequency Band	Degradation Mechanism	Spatial Extent and Duration of Effects*	Comments
VLF	Phase changes, amplitude changes	Hundreds to thousands of miles; minutes to hours	
MF	Absorption of sky waves, defocusing	Hundreds to thousands of miles; minutes to hours	
HF	Absorption of sky waves, loss of support for F-region reflection, multipath interference	Hundreds to thousands of miles; burst region and conjugate; minutes to hours	Daytime absorption larger than nighttime. F-region disturbances may result in new modes, multipath interference
VHF	Absorption, multipath interference, or false targets resulting from resolved multipath radar signals	Few miles to hundreds of miles; minutes to tens of minutes	Fireball and D-region absorption, FPIs circuits may experience attenuation or multipath interference
UHF	Absorption	Few miles to tens of miles; seconds to few minutes	Only important for line-of-sight propagation through highly ionized regions

\*The magnitudes of spatial extent and duration are sensitive functions of detonation altitude and weapon yield.

at an "observation" point at a slant distance  $D$  from the explosion is

$$E_D = \frac{kW}{4\pi D^2} \rho \mu_m e^{-\mu_m M}, \quad (10.138.1)$$

where  $\rho$  is the air density at the observation altitude,  $\mu_m$  is the mass (energy) absorption coefficient in air of the given radiation,<sup>5</sup> and  $M$  is the penetration mass, i.e., the mass of air per unit area between the radiation source and the observation point. This equation may be used for all forms of prompt radiation, using the appropriate value of  $k$  given in Table 10.138. The fraction of the energy radiated as prompt gamma rays is small and its contribution to the electron density is generally less than the for other radiations. If the energy deposited in the air is reradiated or if the source photons or neutrons are scattered and follow a random path before depositing all their energy, equation (10.138.1) must be modified (§ 10.142).

Table 10.138

FRACTION OF EXPLOSION ENERGY  
AS PROMPT RADIATIONS

Radiation	$k$
X rays	0.7
Gamma rays	0.003
Neutrons	0.01

10.139 According to Table 1.45, 1 kiloton TNT equivalent of energy is equal to  $2.6 \times 10^{25}$  million electron volts. Furthermore, about  $3 \times 10^4$  ions

pairs, i.e.,  $3 \times 10^4$  electrons, are produced for each million electron volts of energy absorbed in air (about 34 electron volts are required to produce an ion pair). Consequently, about  $8 \times 10^{29}$  electrons are produced for each kiloton of energy deposited in the air. Hence, the number of free electrons per unit volume,  $N_e$ , is obtained from equation (10.138.1), with  $W$  in kilotons, as

$$N_e = 2.4 \times 10^{18} \frac{kW}{D^2} \rho \mu_m e^{-\mu_m M} \text{ cm}^{-3}, \quad (10.139.1)$$

with  $\rho$  in grams per cubic centimeter,  $\mu_m$  in square centimeters per gram,  $M$  in grams per square centimeter, and  $D$  in miles.

10.140 An expression for  $M$  may be obtained in the following manner. Let  $H_0$  (Fig. 10.140) be the altitude of the explosion point and  $H$  that of the observation point which is at a distance  $D$  from the burst. Then if  $D'$  represents any position between the explosion and the observation point, and  $h$  is the corresponding altitude, the value of  $M$  in appropriate units is given by

$$M = \int_0^D \rho(D') dD' \\ = \frac{D}{H - H_0} \int_{H_0}^H \rho(h) dh,$$

where, in deriving the second form, the curvature of the earth has been neglected. If  $\rho(h)$  is now represented by

<sup>5</sup>The mass absorption coefficient is similar to the mass attenuation coefficient defined in § 8.100, except that it involves the energy absorption coefficient, referred to in the footnote to equation (8.95.1).

approximation. When  $\alpha_d$  is taken equal to  $\alpha_i$ , the electron density,  $N_e(t)$ , as a function of time following a pulse of prompt radiation, can be represented by

$$N_e(t) = \frac{N_e(0)}{1 + \alpha N_e(0)t}.$$

$$\frac{S + Ke^{-(K+S)t}}{S + K}, \quad (10.149.1)$$

for times more than a few seconds after the burst in the daytime, and

$$\frac{N_e(t) \text{ at } 55 \text{ miles}}{N_e(0)} \text{ cm}^{-3} \text{ (nighttime)} \\ \frac{1 + 2 \times 10^{-7} N_e(0)t}{1 + 2 \times 10^{-7} N_e(0)t} \quad (10.150.2)$$

for nighttime conditions.

10.151 Calculations of the decay of electron densities from ionization produced by prompt radiations from a nuclear detonation have been made with a computer using numerical solutions that do not involve the equal-alpha approximation. The results for daytime conditions at a height of 40 miles are shown in Fig. 10.151; they are reasonably consistent with equation (10.150.1) provided the electron density is appreciably larger than the normal value in the ionosphere. Natural ionization sources must be considered when the electron density resulting from prompt radiation has decayed to values comparable to those normally existing at an altitude of 40 miles.

10.152 There are two aspects of Fig. 10.151 that are of special interest. First, it is seen that when the initial electron density,  $N_e(0)$ , is greater than  $10^7$  electrons/cm<sup>3</sup>, the electron density,  $N_e(t)$ , at any time more than about 1

Table 10.150

APPROXIMATE VALUES OF  $\alpha$ ,  $S$ , and  $K$  IN CGS UNITS

Coefficient	40 Miles (daytime)	55 Miles (nighttime)
$\alpha$	$10^{-7}$	$2 \times 10^{-7}$
$S$	0.4	$2 \times 10^{-2}$
$K$	0.8	$2 \times 10^{-3}$

the whole area could be affected almost simultaneously by the EMP from a single high-altitude nuclear explosion.

#### COLLECTION OF EMP ENERGY

**11.16** For locations that are not within or close to the deposition region for a surface or air burst, both the amount and rate of EMP energy received *per unit area* on or near the ground will be small, regardless of the type of nuclear explosion. Hence, for damage to occur to electrical or electronic systems, it would usually be necessary for the energy to be collected over a considerable area by means of a suitable conductor. In certain systems, however, sufficient energy, mainly from the high-frequency components of the EMP, may be collected by small metallic conductors to damage very sensitive components (§ 11.31). The energy is then delivered from the collector (antenna) in the form of a strong current and voltage surge to attached equipment. Actually, the equipment does not have to be attached directly to the col-

lector; the EMP energy can be coupled in other ways (§ 11.27). For example, it is possible for an electric current to be induced or for a spark to jump from the conductor which collects the EMP energy to an adjacent conductor, not connected to the collector, and thence to a piece of equipment.

**11.17** The manner in which the electromagnetic energy is collected from the EMP is usually complex, because much depends on the size and shape of the collector, on its orientation with respect to the source of the pulse, and on the frequency spectrum of the pulse. As a rough general rule, the amount of energy collected increases with the dimensions of the conductor which serves as the collector (or antenna). Typical effective collectors of EMP energy are given in Table 11.17. Deeply buried cables, pipes, etc., are generally less effective than overhead runs because the ground provides some shielding by absorbing the high-frequency part of the energy (see, however, § 11.68).

Table 11.17

#### TYPICAL COLLECTORS OF EMP ENERGY

- Long runs of cable, piping, or conduit
- Large antennas, antenna feed cables, guy wires, antenna support towers
- Overhead power and telephone lines and support towers
- Long runs of electrical wiring, conduit, etc., in buildings
- Metallic structural components (girders), reinforcing bars, corrugated roof, expanded metal lath, metallic fencing
- Railroad tracks
- Aluminum aircraft bodies

#### SUMMARY OF EMP DAMAGE AND PROTECTION

**11.18** The sensitivity of various systems and components to the EMP has

been studied by means of simulators which generate sharp pulses of electromagnetic radiation (§ 11.41 *et seq.*). The results are not definitive because the amount of EMP energy delivered to a

corresponding to this wavelength. Since EMP has a broad spectrum of frequencies, only a portion of this spectrum will couple most efficiently into a specific conductor configuration. Thus, a particular collection system of interest must be examined with regard to its overall configuration as well as to the component configuration. Most practical collector systems, such as those listed in Table 11.17, are complex and the determination of the amount of EMP energy collected presents a very difficult problem. Both computer methods and experimental simulation are being used to help provide a solution.

#### COMPONENT AND SYSTEM DAMAGE

**11.30** Degradation of electrical and electronic system performance as a result of exposure to the EMP may consist of functional damage or operational upset. Functional damage is a catastrophic failure that is permanent; examples are burnout of a device or component, such as a fuse or a transistor, and inability of a component or subsystem to execute its entire range of functions. Operational upset is a temporary impairment which may deny use of a piece of equipment from a fraction of a second to several hours. Change of state in switches and in flip-flop circuits are examples of operational upset. The amount of EMP energy required to cause operational upset is generally a few orders of magnitude smaller than for functional damage.

**11.31** Some electronic components are very sensitive to functional damage (burnout) by the EMP. The actual sensitivity will often depend on the characteristics of the circuit containing the

component and also on the nature of the semiconductor materials and fabrication details of a solid-state device. In general, however, the components listed in Table 11.31 are given in order of decreasing sensitivity to damage by a sharp pulse of electromagnetic energy. Tests with EMP simulators have shown that a very short pulse of about  $10^{-7}$  joule may be sufficient to damage a microwave semiconductor diode, roughly  $5 \times 10^{-2}$  joule will damage an audio transistor, but 1 joule would be required for vacuum tube damage. Systems using vacuum tubes only would thus be much less sensitive to the EMP than those employing solid-state components. The minimum energy required to damage a microammeter or a low-current relay is about the same as for audio transistors.

Table 11.31

#### ELECTRONIC COMPONENTS IN ORDER OF DECREASING SENSITIVITY

- Microwave semiconductor diodes
- Field-effect transistors
- Radiofrequency transistors
- Silicon-controlled rectifiers
- Audio transistors
- Power rectifier semiconductor diodes
- Vacuum tubes

**11.32** As seen earlier, the EMP threat to a particular system, subsystem, or component is largely determined by the nature of the collector (antenna). A sensitive system associated with a poor collector may suffer less damage than a system of lower sensitivity attached to a more efficient collector. Provided the EMP energy collectors are similar in all cases, electrical and electronic systems may be classified in the manner shown

in Table 11.32. However, the amount of energy collected is not always a sufficient criterion for damage. For example, an EMP surge can sometimes serve as a trigger mechanism by producing arcing or a change of state which, in turn, allows the normal operating voltage to cause damage to a piece of equipment. Thus, analysis of sensitivity to EMP

may require consideration of operational upset and damage mechanisms in addition to the energy collected.

#### PROTECTIVE MEASURES

**11.33** A general approach to the examination of a system with regard to its EMP vulnerability might include the

**Table 11.32**  
DEGREES OF SUSCEPTIBILITY TO THE EMP

Most Susceptible	
Low-power, high-speed digital computer, either transistorized or vacuum tube (operational upset)	
Systems employing transistors or semiconductor rectifiers (either silicon or selenium):	
Computers and power supplies	
Semiconductor components terminating long cable runs, especially between sites	
Alarm systems	
Intercom system	
Life-support system controls	
Some telephone equipment which is partially transistorized	
Transistorized receivers and transmitters	
Transistorized 60 to 400 cps converters	
Transistorized process control systems	
Power system controls and communication links	
Less Susceptible	
Vacuum-tube equipment that does not include semiconductor rectifiers:	
Transmitters	Intercom systems
Receivers	Teletype-telephone
Alarm systems	Power Supplies
Equipment employing low-current switches, relays, meters:	
Alarms	Panel indicators and status
Life-support systems	boards
Power system control panels	Process controls
Hazardous equipment containing:	
Detonators	Explosive mixtures
Squibs	Rocket fuels
Pyrotechnical devices	
Other:	
Long power cable runs employing dielectric insulation	
Equipment associated with high-energy storage capacitors	
Inductors	
Least Susceptible	
High-voltage 60 cps equipment:	
Transformers, motors	Rotary converters
Lamps (filament)	Heavy-duty relays, circuit breakers
Heaters	Air-insulated power cable runs

#### THEORY OF THE EMP

**11.71** Unless they happen to be ejected along the lines of the geomagnetic field, the Compton electrons resulting from the interaction of the gamma-ray photons with the air molecules and atoms in the deposition region will be forced to follow curved paths along the field lines.<sup>3</sup> In doing so they are subjected to a radial acceleration and the ensemble of turning electrons, whose density varies with time, emits electromagnetic radiations which add coherently. The EMP produced in this manner from a high-altitude burst—and also to some extent from an air burst—is in a higher frequency range than the EMP arising from local asymmetries in moderate-altitude and surface bursts (§ 11.63).

**11.72** The curves in Figs. 11.70a and b indicate the dimensions of the deposition (source) region, but they do not show the extent of coverage on (or near) the earth's surface. The EMP does not radiate solely in a direction down from the source region; it also radiates from the edges and at angles other than vertical beneath this region. Thus, the effect at the earth's surface of the higher-frequency EMP extends to the horizon (or tangent point on the surface as viewed from the burst). The lower frequencies, however, will extend even beyond the horizon because these electromagnetic waves can follow the earth's curvature (cf. § 10.92). Table 11.72 gives the distances along the surface from ground zero to the tangent point for several burst heights.

**11.73** The peak electric field (and

<sup>3</sup>At higher altitudes, when the atmospheric density is much less and collisions with air atoms and molecules are less frequent, continued turning of the electrons (beta particles) about the field lines leads to the helical motion referred to in §§ 2.143, 10.27.

Table 11.72

#### GROUND DISTANCE TO TANGENT POINT FOR VARIOUS BURST ALTITUDES

Burst Altitude (miles)	Tangent Distance (miles)
62	695
93	850
124	980
186	1,195
249	1,370
311	1,520

its amplitude) at the earth's surface from a high-altitude burst will depend upon the explosion yield, the height of burst, the location of the observer, and the orientation with respect to the geomagnetic field. As a general rule, however, the field strength may be expected to be tens of kilovolts per meter over most of the area receiving the EMP radiation. Figure 11.73 shows computed contours for  $E_{\max}$ , the maximum peak electric field, and various fractions of  $E_{\max}$  for burst altitudes between roughly 60 and 320 miles, assuming a yield of a few hundred kilotons or more. The distances, measured along the earth's surface, are shown in terms of the height of burst. The spatial distribution of the EMP electric field depends on the geomagnetic field and so varies with the latitude; the results in the figures apply generally for ground zero between about 30° and 60° north latitude. South of the geomagnetic equator the directions indicating magnetic north and east in the figure would become south and west, respectively. It is evident from Fig.

**Table 12.09****CASUALTIES AT HIROSHIMA AND NAGASAKI**

Zone	Population	Density (per square mile)		
			Killed	Injured
Hiroshima				
0 to 0.6 mile	31,200	25,800	26,700	3,000
0.6 to 1.6 miles	144,800	22,700	39,600	53,000
1.6 to 3.1 miles	80,300	3,500	1,700	20,000
Totals	256,300	8,500	68,000	76,000
Standardized Casualty Rate: 261,000 (Vulnerable area 9.36 square miles).				
Nagasaki				
0 to 0.6 mile	30,900	25,500	27,300	1,900
0.6 to 1.6 miles	27,700	4,400	9,500	8,100
1.6 to 3.1 miles	115,200	5,100	1,300	11,000
Totals	173,800	5,800	38,000	21,000
Standardized Casualty Rate: 195,000 (Vulnerable area 7.01 square miles).				

**12.10** It is important to note that, although the average population densities in Hiroshima and Nagasaki were 8,500 and 5,800 per square mile, respectively, densities of over 25,000 per square mile existed in areas close to ground zero. For comparison, the average population density for the five boroughs of New York City, based on the 1970 census, is about 24,700 per square mile and for Manhattan alone it is 68,600 per square mile. The population density for the latter borough during the working day is, of course, much higher. The ten next largest U.S. cities have average population densities ranging from 14,900 to 3,000 persons per square mile.

**12.11** The numbers in Table 12.09 serve to emphasize the high casualty potential of nuclear weapons. There are several reasons for this situation. In the first place, the explosive energy yield is very much larger than is possible with conventional weapons, so that both the

area and degree of destruction are greatly increased. Second, because of the high energy yields, the duration of the overpressure (and winds) associated with the blast wave, for a given peak overpressure, is so long that injuries occur at overpressures which would not be effective in a chemical explosion. Third, the proportion of the explosive energy released as thermal radiation is very much greater for a nuclear weapon; hence there is a considerably larger incidence of flash burns. Finally, nuclear radiation injuries, which are completely absent from conventional explosions, add to the casualties.

**12.12** The data in the table also show that more than 80 percent of the population within 0.6 mile (3170 feet) from ground zero were casualties. In this area the blast wave energy, thermal exposure, and initial nuclear radiation were each sufficient to cause serious injury or death. Beyond about 1.6 miles, however, the chances of survival

was less for persons in residential (wood-frame and plaster) structures and least of all for those in concrete buildings. These facts emphasize the influence of circumstances of exposure on the casualties produced by a nuclear weapon and indicate that shielding of some type can be an important factor in survival. For example, within a range of 0.6 mile from ground zero over 50 percent of individuals in Japanese-type homes probably died of nuclear radiation effects, but such deaths were rare among persons in concrete buildings within the same range. The effectiveness of concrete structures in providing protection from injuries of all kinds is apparent from the data in Table 12.17; this gives the respective average distances from ground zero at which there was 50-percent survival (for at least 20 days) among the occupants of a number of buildings in Hiroshima. School personnel who were indoors had a much higher survival probability than those who were outdoors at the times of the explosions.

**Table 12.17****AVERAGE DISTANCES FOR 50-PERCENT SURVIVAL AFTER 20 DAYS IN HIROSHIMA**

	Approximate Distance (miles)
Overall	0.8
Concrete buildings	0.12
School personnel:	
Indoors	0.45
Outdoors	1.3

**CAUSES OF INJURIES AMONG SURVIVORS**

**12.18** From surveys made of a large number of Japanese, a fairly good idea

has been obtained of the distribution of the three types of injuries among those who became casualties but survived the nuclear attacks. The results are quoted in Table 12.18; the totals add up to more than 100 percent, since many individuals suffered multiple injuries.

**Table 12.18****DISTRIBUTION OF TYPES OF INJURY AMONG SURVIVORS**

Injury	Percent of Survivors
Blast (mechanical)	70
Burns (flash and flame)	65
Nuclear radiation (initial)	30

**12.19** Among survivors the proportion of indirect blast (mechanical) injuries due to flying missiles and motion of other debris was smallest outdoors and largest in certain types of industrial buildings. Patients were treated for lacerations received out to 10,500 feet (2 miles) from ground zero in Hiroshima and out to 12,500 feet (2.2 miles) in Nagasaki. These distances correspond roughly to those at which moderate damage occurred to wood-frame houses, including the shattering of window glass.

**12.20** An interesting observation made among the Japanese survivors was the relatively low incidence of serious mechanical injuries. For example, fractures were found in only about 4 percent of survivors. In one hospital there were no cases of fracture of the skull or back and only one fractured femur among 675 patients, although many such injuries must have undoubtedly occurred. This was attributed to the fact that persons who suffered severe concussion or

fractures were rendered helpless, particularly if leg injuries occurred, and, along with those who were pinned beneath the wreckage, were trapped and unable to seek help or escape in case fire ensued. Such individuals, of course, did not survive.

#### CASUALTIES AND STRUCTURAL DAMAGE

**12.21** For people who were in buildings in Japan, the overall casualties were related to the extent of structural damage, as well as to the type of structure (§ 12.17). The data in Table 12.21 were obtained from a study of 1,600 Japanese who were in reinforced-concrete buildings, between 0.3 and 0.75 mile from ground zero, when the nuclear explosions occurred. At these distances fatalities in the open ranged from about 90 to 100 percent, indicating, once more, that people were safer inside buildings, even when no special protective action was taken because of the lack of warning. There may have been an increase of casualties in buildings from debris etc., but this was more than compensated by the reduction due to

shielding against the initial nuclear radiation and particularly from the thermal pulse.

**12.22** In two concrete buildings closest to ground zero, where the mortality rate was 88 percent, about half the casualties were reported as being early and the other half as delayed. The former were attributed to a variety of direct and indirect blast injuries, caused by overpressure, structural collapse, debris, and whole-body translation, whereas the latter were ascribed mainly to burns and initial nuclear radiation. Minor to severe but nonfatal blast injuries no doubt coexisted and may have contributed to the delayed lethality in many cases. At greater distances, as the threat from nuclear radiation decreased more rapidly than did that from air blast and thermal radiation, the proportion of individuals with minor injuries or who were uninjured increased markedly. The distribution of casualties of different types in Japanese buildings was greatly influenced by where the people happened to be at the time of the explosion. Had they been forewarned and knowledgeable about areas of relative hazard and safety, there would probably have

Table 12.21  
CASUALTIES IN REINFORCED-CONCRETE BUILDINGS IN JAPAN RELATED TO STRUCTURAL DAMAGE

Structural Damage	Killed Outright	Percent of Individuals		
		Serious Injury (hospital- ization)	Light Injury (no hospi- talization)	No Injury Reported
Severe damage	88	11	—	1
Moderate damage	14	18	21	47
Light damage	8	14	27	51

lethality are average pressures obtained by extrapolation from animal data to man; the variability of the results is indicated by the numbers in parentheses. Rupture of the normal eardrum is apparently a function of the age of the individual as well as of the effective blast pressure. Failures have been recorded at overpressures as low as 5 pounds per square inch ranging up to 40 or 50 pounds per square inch. The values in Table 12.38 of the effective peak overpressures for eardrum rupture are based on relatively limited data from man and animals.

#### INDIRECT BLAST INJURIES

**12.39** Indirect blast injuries are associated with (1) the impact of missiles, either penetrating or nonpenetrating (secondary effects), and (2) the physical displacement of the body as a whole (tertiary effects). The wounding potential of blast debris depends upon a number of factors; these include the impact (or striking) velocity, the angle

at which impact occurs, and the size, shape, density, mass, and nature of the moving objects. Furthermore, consideration must be given to the portion of the body involved in the missile impact, and the events which may occur at and after the time of impact, namely, simple contusions and lacerations, at one extreme, or more serious penetrations, fractures, and critical damage to vital organs, at the other extreme.

**12.40** The hazard from displacement depends mainly upon the time and distance over which acceleration and deceleration of the body occur. Injury is more likely to result during the latter phase when the body strikes a solid object, e.g., a wall or the ground. The velocity which has been attained before impact is then significant. This is determined by certain physical parameters of the blast wave, as mentioned below, as well as by the orientation of the body with respect to the direction of motion of the wave. The severity of the damage depends on the magnitude of the impact velocity, the properties of the impact

Table 12.38  
TENTATIVE CRITERIA FOR DIRECT (PRIMARY) BLAST EFFECTS IN MAN FROM FAST-RISING, LONG-DURATION PRESSURE PULSES

Effect	Effective Peak Pressure (psi)
Lung Damage:	
Threshold	12 (8-15)
Severe	25 (20-30)
Lethality:	
Threshold	40 (30-50)
50 percent	62 (50-75)
100 percent	92 (75-115)
Eardrum Rupture:	
Threshold	5
50 percent	15-20 (more than 20 years old)
	30-35 (less than 20 years old)

## BIOLOGICAL EFFECTS

Table 12.43

## VELOCITIES, MASSES, AND DENSITIES OF MISSILES

Missile	Peak Overpressure (psi)	Median Velocity (ft/sec)	Median Mass (grams)	Maximum Number per Sq Ft
Glass	1.9	108	1.45	4.3
Glass	3.8	168	0.58	159
Glass	3.9	140	0.32	108
Glass	5.0	170	0.13	388
Stones	8.5	286	0.22	40

tion was 5.3 pounds per square inch. The dummy traveled 13 feet before striking the ground and then slid or rolled another 9 feet. A prone dummy, however, did not move under the same conditions. The foregoing results were obtained in a situation where the blast wave was nearly ideal, but in another test, at a peak overpressure of 6.6 pounds per square inch, where the blast wave was nonideal (§ 3.79), both standing and prone dummies suffered considerably greater displacements. Even in such circumstances, however, the displacement of over 125 feet for the prone dummy was much less than that of about 250 feet for the standing one. The reason for the greater displacement of the standing dummy is that it acquired a higher velocity.

**12.45** In order to study the displacements of moving objects, field tests have been made by dropping animal cadavers, including guinea pigs, rabbits, goats, and dogs, and stones and concrete blocks onto a flat, hard surface from a vehicle traveling between 10 and 60 miles per hour (14.7 to 88 feet per second). For a given initial velocity, the stopping distance for the animals increased somewhat with the mass, and a

relationship was found to represent the stopping distance as a function of velocity applicable to the animals over a wide range of mass (§ 12.239). One reason for the consistency of the data is probably that all the animals assumed a rolling position about their long axis regardless of the initial orientation. The animals remained relatively low to the ground and bounced very little. By contrast, stones and concrete blocks bounced many times before stopping; the data were not sensitive to mass, depended more on orientation, and were more variable than the results obtained with animals. On the whole, the stopping distances of the blocks and stones were greater for a given initial velocity. One of the conclusions drawn from the foregoing tests was that a person tumbling over a smooth surface, free from rocks and other hard irregularities, might survive, even if the initial velocity is quite high, if he could avoid head injury and did not flail his limbs.

## MISSILE AND DISPLACEMENT INJURY CRITERIA

**12.46** Velocity criteria for the production of skin lacerations by penetrat-

## BLAST INJURIES

555

ing missiles, e.g., glass fragments, are not known with certainty. Some reliable information is available, however, concerning the probability of penetration of the abdominal wall by glass. The impact velocities, for glass fragments of different masses, corresponding to 1, 50, and 99 percent penetration probability are recorded in Table 12.46.

**12.47** The estimated impact velocities of a 10-gram (0.35-ounce) glass missile required to produce skin lacerations and serious wounds are summarized in Table 12.47. The threshold

value for skin lacerations is recorded as 50 feet per second and for serious wounds it is 100 feet per second.

**12.48** Little is known concerning the relationship between mass and velocity of nonpenetrating missiles that will cause injury after impact with the body. Studies with animals showed that fairly high missile velocities are required to produce lung hemorrhage, rib fractures, and early mortality, but quantitative data for man are lacking. No relationship has yet been developed between mass and velocity of nonpene-

Table 12.46

## PROBABILITIES OF GLASS FRAGMENTS PENETRATING ABDOMINAL WALL

Mass of Glass Fragments (grams)	Probability of Penetration (percent)		
	1	50	99
Impact Velocity (ft/sec)			
0.1	235	410	730
0.5	160	275	485
1.0	140	245	430
10.0	115	180	355

Table 12.47

## TENTATIVE CRITERIA FOR INDIRECT (SECONDARY) BLAST EFFECTS FROM PENETRATING 10-GRAM GLASS FRAGMENTS\*

Effect	Impact Velocity (ft/sec)
Skin laceration: Threshold	50
Serious wounds: Threshold 50 percent Near 100 percent	100 180 300

\*Figures represent impact velocities with unclothed skin. A serious wound is arbitrarily defined as a laceration of the skin with missile penetration into the tissues to a depth of 1 cm (about 0.4 inch) or more.

trating missiles that will cause injury as a result of impacts with other parts of the body wall, particularly near the spine, kidney, liver, spleen and pelvis. It appears, however, that a missile with a mass of 10 pounds striking the head at a velocity of about 15 feet per second or more can cause skull fracture. For such missiles it is unlikely that a significant number of dangerous injuries will occur at impact velocities of less than 10 feet per second. The impact velocities of a 10-pound missile for various effects on the head are given in Table 12.48.

**12.49** Although there may be some hazard associated with the accelerative phase of body displacement (translation) by a blast wave, the deceleration, particularly if impact with a solid object is involved, is by far the more significant. Since a hard surface will cause a more serious injury than a softer one, the damage criteria given below refer to perpendicular impact of the displaced body with a hard, flat object. From various data it is concluded that an im-

pact velocity of 10 feet per second is unlikely to be associated with a significant number of serious injuries; between 10 and 20 feet per second some fatalities may occur if the head is involved; and above 20 feet per second, depending on trauma to critical organs, the probabilities of serious and fatal injuries increase rapidly with increasing displacement velocity. Impact velocities required to produce various indirect (tertiary) blast effects are shown in Table 12.49. The curves marked "translation near structures" in Fig. 12.49 may be used to estimate ground distances at which 1 percent and 50 percent casualties would be expected, as functions of height of burst, for a 1-kiloton explosion.<sup>5</sup> Based on tests with animals, the criteria for 1 and 50 percent casualties were somewhat arbitrarily set at impact velocities of 8 and 22 feet per second, respectively. The results in Fig. 12.49 may be extended to other burst heights and yields by using the scaling law given in the example facing the figure.

**Table 12.48**  
TENTATIVE CRITERIA FOR INDIRECT BLAST EFFECTS INVOLVING  
NONPENETRATING 10-POUND MISSILES

Effect	Impact Velocity (ft/sec)
Cerebral Concussion:	
Mostly "safe"	10
Threshold	15
Skull Fracture:	
Mostly "safe"	10
Threshold	13
Near 100 percent	23

<sup>5</sup>In this connection, a casualty is defined as an individual so injured that he would probably be a burden on others. Some of the casualties would prove fatal, especially in the absence of medical care.

**Table 12.49**  
TENTATIVE CRITERIA FOR INDIRECT (TERTIARY) BLAST EFFECTS INVOLVING  
IMPACT

Effect	Impact Velocity (ft/sec)
<b>Standing Stiff-Legged Impact:</b>	
Mostly "safe"	
No significant effect	< 8
Severe discomfort	8-10
Injury	
Threshold	10-12
Fracture threshold (heels, feet, and legs)	13-16
<b>Seated Impact:</b>	
Mostly "safe"	
No effect	< 8
Severe discomfort	8-14
Injury	
Threshold	15-26
<b>Skull Fracture:</b>	
Mostly "safe"	10
Threshold	13
50 percent	18
Near 100 percent	23
<b>Total Body Impact:</b>	
Mostly "safe"	10
Lethality threshold	21
Lethality 50 percent	54
Lethality near 100 percent	138

**12.50** Evaluation of human tolerance to decelerative tumbling during translation in open terrain is more difficult than for impact against a rigid surface described above. Considerably fewer data are available for decelerative tumbling than for body impact, and there is virtually no human experience for checking the validity of extrapolations from observations on animal cadavers. Tests have been made with goats, sheep, and dogs, but for humans the information required to derive reliable hazards criteria for decelerative

tumbling are still not adequate. The initial velocities at which 1 and 50 percent of humans are expected to become casualties as a result of decelerative tumbling have been tentatively estimated to be 30 and 75 feet per second, respectively. The curves in Fig. 12.49 marked "translation over open terrain" are approximate, but they may be used to provide a general indication of the range within which casualties might occur from decelerative tumbling due to air blast from surface and air bursts.

(Text continued on page 560.)

**Table 12.108**  
**SUMMARY OF CLINICAL EFFECTS OF ACUTE IONIZING RADIATION DOSES**

Range	0 to 100 rads Subclinical range	100 to 1,000 rads Therapeutic range			Over 1,000 rads Lethal range	
		100 to 200 rads	200 to 600 rads	600 to 1,000 rads	1,000 to 5,000 rads	Over 5,000 rads
Incidence of vomiting	None	100 rads: infrequent 200 rads: common	Clinical surveillance	Therapy effective	Therapy promising	Therapy palliative
						100%
Initial Phase	Onset	—	3 to 6 hours	½ to ½ hour	5 to 30 minutes	Almost immediately**
	Duration	—	≤ 1 day	≤ 2 days	≤ 1 day	Almost immediately**
Latent Phase	Onset	—	≤ 1 day	1 to 2 days	≤ 1 day*	Almost immediately**
	Duration	—	≤ 2 weeks	1 to 4 weeks	0 to 7 days*	
Final Phase	Onset	—	10 to 14 days	1 to 4 weeks	0 to 10 days	Almost immediately**
	Duration	—	4 weeks	1 to 8 weeks	1 to 4 weeks	
Leading organ			Hematopoietic tissue	Gastrointestinal tract	Central nervous system	
Characteristic signs	None below 50 rads	Moderate leukopenia	Severe leukopenia; purpura; hemorrhage; infection. Epilation above 300 rads.	Diarrhea; fever; disturbance of electrolyte balance. Convulsions; tremor; ataxia; lethargy.		
Critical period post-exposure	—	—	—	1 to 6 weeks	2 to 14 days	1 to 48 hours

#### NUCLEAR RADIATION INJURY

Therapy	Reassurance	Reassurance; hematologic surveillance.	Blood transfusion; antibiotics.	Consider bone marrow transplantation.	Maintenance of electrolyte balance.	Sedatives
Prognosis	Excellent	Excellent	Guarded	Guarded	Hopeless	
Convalescent period	None	Several weeks	1 to 12 months	Long	—	
Incidence of death	None	None	0 to 90%	90 to 100%	100%	
Death occurs within	—	—	2 to 12 weeks	1 to 6 weeks	< 1 day to 2 days	
Cause of death	—	—	Hemorrhage; infection	Circulatory collapse	Respiratory failure; brain edema.	

\*At the higher doses within this range there may be no latent phase.

\*\*Initial phase merges into final phase, death usually occurring from a few hours to about 2 days; this chronology is possibly interrupted by a very short latent phase.

## BIOLOGICAL EFFECTS

except that the latter are soon visible whereas the effects of beta particles may not be seen for three or four weeks.

**12.246** The damage to the cattle at the TRINITY site was described as the development of zones of thickened and hardened skin which appeared as plaques and cutaneous horns. After 15 years, three of the exposed cows developed scale-like carcinomas of the skin in the affected regions, but it is not entirely clear that they were induced by radiation. In areas less severely affected, there was some loss and graying of the hair. The location of these cattle with respect to ground zero is not known, but it is estimated that the whole-body gamma radiation dose was about 150 rems, although the skin dose may have been very much larger. There was no evidence of radiation damage on the lower surfaces of the body that might have been caused by exposure from fallout on the ground.

**12.247** Information concerning the possible effects of fallout on farm animals under various conditions has been obtained from studies with simulated fallout sources. Three main situations of interest, depending on the location of the animals, are as follows:

1. In a barn: whole-body exposure

to gamma rays from fallout on the roof and the surrounding ground.

2. In a pen or corral: whole-body exposure to gamma rays from fallout on the ground and exposure of the skin to beta particles from fallout deposited on the skin.

3. In a pasture: whole-body exposure to gamma rays from fallout on the ground, exposure of the skin to beta particles, and exposure of the gastrointestinal tract from fallout on the grass.

The exposure to gamma rays is simulated by means of an external cobalt-60 source. Skin irradiation is achieved by attaching to the back of the animal a flexible source of beta particles. Finally, the internal exposure is simulated by adding to the animal's feed a material consisting of yttrium-90 fused to 88-175 micrometers particles of sand, giving a specific activity of 10 microcuries per gram of sand. This product is considered to be representative of the beta radiation from the fallout produced by a land-surface detonation.

**12.248** Observations have been made on animals exposed to whole-body gamma radiation alone (barn) or in combination with skin exposure (pen or corral) or with exposure of the skin and the intestinal tract (pasture) at dose rates

Table 12.248

ESTIMATED LIVESTOCK LETHALITY ( $LD_{50/60}$ ) FROM FALLOUT

Animals	Total Gamma Exposure (roentgens)		
	Barn	Pen or Corral	Pasture
Cattle	500	450	180
Sheep	400	350	240
Swine	640	600*	550*
Horses	670	600*	350*
Poultry	900	850*	800*

\* No experimental data available; estimates are based on grazing habits, anatomy, and physiology of the species.